ELECTROCHEMICAL AND MECHANICAL

PROPERTIES STUDIES

ON MG-RICH FLEXIBLE SULFUR-CONTAINING

POLYMER PRIMERS

A Thesis
Submitted to The Graduate Faculty
of the
North Dakota State University
of Agriculture and Applied Science

By

Tiantian Chen

In Partial Fulfillment of the Requirements
for the Degree of
MASTER OF SCIENCE

Major Department:
Coatings and Polymeric Materials

March 2010

Fargo, North Dakota

North Dakota State University
Graduate School

Title

Electrochemical and Mechanical Properties' Studies of Flexible Mg-rich Primers

By

Tiantian Chen

The Supervisory Committee certifies that this **_disquisition_** complies with North Dakota State University's regulations and meets the accepted standards for the degree of

MASTER OF SCIENCE

ABSTRACT

Chen, Tiantian, M. S., Department of Coatings and Polymeric Materials, College of Science and Mathematics, North Dakota State University, March 2010. Electrochemical and Mechanical Properties Studies of Flexible Mg-rich Primers. Major Professor: Dr. Gordon P. Bierwagen.

The coating systems for military aircraft must protect the aluminum skin and frame, and associated fastening and joining from corrosion in a variety of aggressive environments. Excessive grinding is often needed to remove the corrosion products at the cracks formed around the seams and fasteners on the aircraft resulting from poor system flexibility of coatings, which causes high maintenance cost and damages the integrity of the aircraft's body. Thus the U.S. Air Force wants to develop an advanced performance coating system with a primer that can provide superior flexibility and good corrosion protection. Currently commercialized magnesium-rich corrosion protection primers were initially developed from some epoxy-amine coating systems, the most common polymer system for aircraft primer use. But the primers were developed under the old specification, which cannot meet the "ideal" goals of the Air Force. Thus, as a carefully selected alternate, polysulfide modified polymers, which have lowest gas permeability, outstanding oil resistance and UV resistance, and especially great flexibility, are being examined as candidate materials.

In this research, a number of accelerated laboratory testing methods were applied to measure the electrochemical and mechanical properties of the modified Mg-rich primers which are based on polysulfide modified polymer as binder. Electrochemical measurement results and visual inspections show that the Mg-rich flexible primer has better or equal

corrosion protection performance versus a standard epoxy-based Mg-rich primer with the same PVC. The flexibility of the newly formulated Mg-rich primer was also indicated by the results of a variety of empirical testings and instrumental characterizations. Meanwhile, the weathering impact introduced by the laboratory accelerated exposure cannot compromise the superiority of the flexible Mg-rich primers. Based on the results found, future work will be focused on creating a new formulate method or making some modification of the sulfur-containing polymer's structure to achieve a really low VOC.

ACKNOWLEDGEMENTS

First and foremost I would like to give my sincerest gratitude to my graduate advisor, Dr. Gordon Bierwagen, who has guided me throughout my thesis with his great patience and support. Without his effort and encouragement, this thesis could not have been completed.

I would like to thank the many people who have helped me on my research and thesis writing. Especially, I am grateful to Jinhai Wang, Brad Halverson and Heidi Docktor for the help on the experimental instruments I used in the work.

I acknowledge the help from the Chevron Phillips Company, the provider of the sulfur-containing resins used in the research, and Air Force Office of Scientific Research (AFOSR) for the financial support on this research.

I also would like to thank my family members, especially my wife, Qing Liu, for supporting and encouraging me to pursue the degree. Her encouragement was crucial for me to finish this degree.

TABLE OF CONTENTS

LIST OF TABLES

LIST OF FIGURES

CHAPTER 1. INTRODUCTION

When two different metals are joined in a corrosive environment, the more reactive one will oxidize preferentially, and meanwhile provide cathodic protection to the nobler one to keep it from corrosion. This scientific concept has been applied to the corrosion protection of steel substrate in the use of zinc-rich sacrificial coatings, which has been in place since the 1940s.[1] By analogy, after several year of studies and applications, magnesium-rich galvanic sacrificial primers have demonstrated their importance among the chromium-free methods of protecting aluminum and its alloys from corrosion, especially with respect to high-strength and low-density aircraft Al alloys.[2,3] Nevertheless, corrosion protection is not the only important parameter of aircraft coatings. The failure of the coating around the fasteners and seams because of lack of flexibility in the coating system can lead to corrosion and excessive grinding which is done to remove corrosion products. Thus to achieve complete protective performance on aircraft primers, flexibility is another performance factor for total corrosion corrosion protection.

In the 19th century, sulfur was first introduced into polymers with the invention of the vulcanization process, which provided the industrial world with a new durable and elastic material: organic rubber. In 1927, a new sulfur-containing synthetic rubber, polysulfide, which was then commercially produced by Thiokol Chemical Corporation in 1929, was discovered by J. C. Patrick.[4] The polysulfide elastomer satisfied the increasing demand for fuel resistance products that was occurring during the Second World War, and dominated the sealant market in 1950's, because of its excellent chemical resistance and UV stability. However, possibly due to its powerful odor along with the need for strong

solvents, polysulfide fell out of use by chemists and chemical engineers, which resulted in little progress in polysulfide chemistry after the 1980's. Moreover, its leading position in the U. S. sealant market has been replaced by silicone and polyurethane sealants.[5]

In this research, a novel flexible polysulfide polymer combined with the corrosion protection technology of Mg-rich coatings was examined for its ability to improve the performance of Mg-rich aircraft primers. Accelerated weathering testings, including ASTM B117 continuous salt fog spray, ASTM D 5894 Prohesion and UV cyclic weathering, were used to characterize coatings' corrosion protective lifetime during exposure.[6] Electrochemical characterization of the system was obtained by using electrochemical impedance spectroscopy (EIS) and electrochemical noise methods (ENM). Data on mechanical properties were collected by dynamic mechanical thermal analysis (DMTA) and indentation studies. Some other characterizations were also taken according to ASTM standards.

In the second chapter, a review is made conceiving corrosion and Mg-rich coatings, and flexibility and polysulfide elastomers. Then a description of experimental methods which were utilized in this research is given in Chapter 3. In the fourth and fifth part, the results of electrochemical and mechanical experiments are presented and discussed. The conclusions are given in Chapter 6.

1.1. References

1.   U. R. Evans, J. E. O. Mayne, Protection by paints richly pigmented with Zn dust. *Society of Chemical Industry Journal* **1944**, *22*, 109-110.

2.   M. E. Nanna, G. P. Bierwagen, Mg-Rich Coatings: A New Paradigm for Cr-Free Corrosion Protection of Al Aerospace Alloys. *Journal of Coating Technology Research* **2004,** (1), 69-81.

3.   D. Battocchi, G. P. Bierwagen, A. Stamness, D. Tallman, A. Simões, Magnesium-rich primers for chromate-free protective systems on Al 2024 and Al 7075. L. Fedrizzi, Ed. Woodhead Publishing, Ltd: Cambridge, UK, 2007; pp 63-71.

4.   J. C. Patrick, N. M. Mnookin Vulcanizable Compounds and Volcanized Products Derived Therefrom. 1,890,231, 1932.

5.   R. M. Evans, Urethane Construction Sealants. In *Polyurethane Sealants*, Evans, Ed. Technomic Publishing: Lancaster, PA, 1993; pp 1-22.

6.   G. Bierwagen, D. Tallman, J. Li, L. He, C. Jeffcoate, EIS studies of coated metals in accelerated exposure. *Progress in Organic Coatings* **2003,** *46* (2), 148-157.

CHAPTER 2. LITERATURE REVIEW

2.1. Overview of Mg-Rich Coatings

When two different metals are joined in a corrosive environment, the more reactive one acting as anode tends to corrode preferentially, making the chemically more noble metal the cathode, giving it protection against corrosion. Coatings can primarily provide a physical barrier between the substrate and the corrosive environment, as well as cosmetic appearance. What is more, cathodic protection has been applied to the corrosion protection of steel substrate by using zinc-rich sacrificial coatings, which have been widely studied and used as one of the most maturely developed metal-rich primers for the past few decades.[1-8]

The effectiveness of the zinc-rich primers mainly depends on having the pigment volume concentration (PVC) above the critical pigment volume concentration (CPVC), so that the high level of pigmentation provides for electrical contact between the close-packed zinc particles. Zinc hydroxide and zinc carbonate, which are produced by consuming the zinc particles in the primer, may provide passivation protection to the steel substrate.[2, 3, 6]

The CPVC is shortly defined as "the pigment volume concentration (PVC) where there is just sufficient binder to provide a complete adsorbed layer on the pigment surfaces and to fill all of the interstices between the particles in a close-packed system." Below the CPVC, the pigment particles are not close-packed and the binder occupies the volume between the particles in the film; above CPVC, the pigment particles are nearly close-packed, but there is not enough binder to occupy all the volume between the particles,

4

resulting in voids in the film. Many properties of coating films change abruptly at the point of the CPVC, which includes density, tensile strength, adhesion, stain resistance, and gloss, etc..[9-11]

Aluminum and its alloys have been extensively used in a wide variety of markets, including building and construction, transportation, packaging, and so on, since the aluminum industry started evolving a century ago. However, the galvanic corrosion could be very serious if a more reactive metal is alloyed with aluminum. Thus the protection of aluminum and its alloys against corrosion is becoming a more important issue in connection with the prosperity of aluminum alloy market, especially in the aerospace industry. Aluminum alloys AA2024-T3 and AA7075-T6 are widely used in the aerospace industry for their high strength and low density. However, the intermetallic precipitates with Al, Fe, Cu, Mn, etc. formed during manufacturing treatment are responsible for the generation of the electrochemical potential differences along the surface, which makes the aluminum alloys vulnerable to localized corrosion.[12, 13] Currently most US Air Force (USAF) coatings on the aircrafts' bodies are subjected to chromate-based substrate pretreatment, which can provide excellent paint bonding, corrosion resistance and, particularly, the ability of self-healing. The most common Al alloy surface pretreatment (e.g. Alodine® 1200 pretreatment) is an acid bath containing Cr^{6+} ions, while $SrCrO_4$ pigments are used in the primer coating. The hexavalent chromium ions involved in the processes are very toxic to environmental and occupational health. The use of the chromate-based corrosion protection system is being phased out by newly established and even more restrict regulations.[14]

A variety of techniques were developed and researched to replace the Cr-based aluminum alloy substrate pretreatment. Like the Zn-rich primer, after years of studies and applications, magnesium-rich galvanic sacrificial primers gradually showed their importance among the methods of protecting aluminum and its alloy from corrosion, especially with respect to high-strength and low-density aircraft Al alloys. For the first time, Bierwagen and Nanna in 2004[15] described the usage of Mg-rich primers in the first successful totally chromate-free coating system for aerospace Al alloys. As a competitive replacement of the environmentally unfriendly chromate-based corrosion protection system, the protective mode of Mg-rich primers has been studied and proved to be similar to those that have be associated with Zinc-rich primers by Bierwagen and co-workers.[13, 16-19] The sacrificial corrosion protection mechanism of Mg-rich primers is described as a two-stage process: in the first stage, magnesium pigments are consumed as cathodic protection to prevent corrosion of aluminum, whereas at a later stage the precipitation of a porous layer of magnesium oxide was formed to provide barrier protection. A newly published research article has reported that Mg alloy pigments can be a possible replacement of Mg pigment.[20] Though much effort has been already made to investigate the unique anti-corrosion coating, most research focused on the electrochemical properties and interpretation of electrochemical measurement data, and the techniques deployed to study the Mg-rich primers were quite limited to the electrochemical corrosion measurements, such as electrochemical impedance spectroscopy (EIS), scanning vibrating electrochemical technique (SVET), scanning electrochemical microscopy (SECM)[19, 21] and so on. In addition to these techniques, there is still much work that can be done to explore the Mg-rich coatings.

2.2. Introduction to Flexibility in Polymers

Indeed, the term "flexibility" discussed here can be understood as the properties of deformation and durability of materials based on short-term responses. The deformation requires evaluating stiffness of the material in the elastic and non-elastic region, and the durability requires evaluating toughness, i.e., ultimate properties, of the material at failure.[22] A wide variety of mechanical tests that are available for measuring "flexibility" are categorized below. Discussions of two experiments are given here, although there are many others that can be included as well.

Table 1. Mechanical end-use properties.[22]

Stiffness	Toughness
Stress-strain	Ductile and brittle fracture
Modulus	Stress and elongation at break
Yield stress	Impact strength

A simple rubber band is able to be stretched several times as long as its original length, and also able to snap back to its original dimension substantially when being released. By contrast, a steel wire can hardly be stretched beyond 1% extension at room temperature, but is more likely to undergo an irreversible deformation and then break under even very little elongation when reaching its break point. The ability to deform under certain force and subsequently to return to its original shape and size when the force is removed is termed flexibility, i.e., elasticity. In physics, the force that causes deformation (e.g. bending, stretching, or compression), is called the stress, and the amount of

deformation is called the strain. Hooke's law of elasticity describes the ideal proportional

relationship between the load added to a spring and the spring's extension

$$F = -kx$$...................................Equation 1

where F, k and x stand for the force added on the spring (usually in newtons), the spring

constant (usually in N/m) and the extension (usually in meters), respectively. As the spring

constant, k, is simply the physical factor of an ideal spring, the quotient obtained by

dividing the stress by the strain is one of the typical way to characterize the flexibility (or

elasticity) of the material, termed the elastic modulus or Young's modulus. Young's

modulus, E, can be written as follows:

$$E = \sigma/\varepsilon$$...................................Equation 2

where σ and ε represent the stress and the strain. The higher the value of E, the stiffer the

material is, and the more difficult it is to stretch the material.[23]

As mentioned above, Hooke's law describes the proportional relationship of the

ideal elastic material. For real polymers, the stress-strain curve can seldom be linear,

because polymeric materials are usually viscoelastic. Unlike an ideal elastic material, even

if the deformative stress is released, the deformation of an ideal viscous material is

permanent. Viscous deformation is time dependent while elastic deformation is not. Figure

1 shows a schematic stress-strain curve, which was plotted based on a typical polymer

coatings film elongated at a constant rate. The initial slope of the stress-strain curve

demonstrates Young's modulus of the polymer. As the strain increases, it reaches a yield

point, which is the maximum stress (or strain) that can be added to the polymeric material and then the polymeric material can instantaneously return to its original dimension when the stress is removed. The whole curve is divided into the elastic and the plastic regions exactly at this point, where the deformation is no longer time-independent if the strain continues increasing. The plastic region clearly shows the polymer's character of viscoelasticity, a nonlinear extensive elongation under a nearly constant stress, until the polymer material breaks at the point (S_u) of ultimate tensile strength. The toughness is defined by the area below the curve.
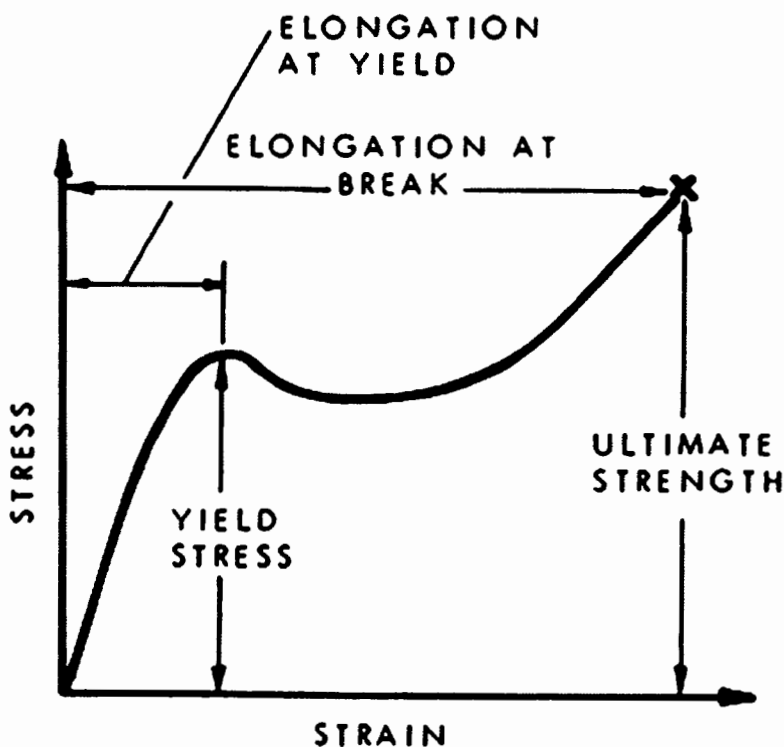
Figure 1. Generalized tensile stress-strain curve for polymeric materials.[24]

Figure 1 schematically illustrates a stress-strain curve of a tough plastic, such as semicrystallized polyethylene. However, different from the curve's type shown, elastomers

9

may have a peculiar nonlinear curve. Polymeric elastomers chemically have hard and stiff domains surrounded by soft, long and randomly coiled domains. This structure determines that the stress applied on the elastomers can be re-distributed by re-configuring the long and spring-like polymer chains.[25] This property enables some elastomers to be elongated up to several hundred percent.[26] It is important to mention that more than one measurement is needed to obtain statistically significant data, due to the fact that the stress-strain curves are depending ultimately on the local stress concentration and coating heterogeneity, such as impurities and air voids, in coating films.

Different from the measurement of the static modulus, dynamic mechanical properties are measured under cyclical or repetitive motions of stress and strain. Elastic materials, an ideal spring for example, convert mechanical work into potential energy, which is recoverable. On the other hand, viscous materials, like liquids, flow if subjected to a stress; they do not store any energy but dissipate it almost entirely as heat instead. Viscoelastic polymers possess both elastic and viscous properties. The storage modulus and loss modulus of the polymers obtained by the dynamic mechanical measurement are defined as a measure of the energy stored elastically during deformation and a measure of the energy converted into heat, respectively. The complex Young's modulus, E, can be written as:

$$E = |E^*| = |E' + iE''|................Equation\ 3$$

where E' symbolizes storage modulus, E" symbolizes loss modulus, and i standard imaginary unit.

2.3. General Overview on Polysulfide and Sulfur-Containing Polymers

Sulfur is widely distributed through the world. In the middle of 19th century, sulfur was first introduced into the artificial macromolecule world by the invention of the vulcanization process found by Goodyear, which gave the industrial world a new durable and elastic material: organic rubber.[27] The study of rubber and rubber elasticity theory began a couple of decades earlier than the invention of the vulcanization process, though a more realistic understanding of the molecular structure of polymer had not been established at that time. Indeed, vulcanization is the chemical crosslinking process that helps natural rubber achieve dimensional stability, reduce creep and plastic flow, and increase toughness. This began to be understood in 1920's due to Staudinger's research on the theory of the long-chain structure of polymers.

In the early years, vulcanized natural rubber was the only available elastomer. In 1927, J. C. Patrick discovered and patented a sulfur-containing synthetic rubber: Thiokol® polysulfide,[28] which then was put into commercial production by Thiokol Chemical Corporation in 1929. During World War II, newly developed liquid polysulfides (LP) were extensively used as sealants in aircraft fuel tanks due to their sound chemical resistance and UV stability.[29-34]

Polysulfide polymers are produced by the reaction between alkyl chlorides and sodium polysulfide that was actually discovered by Patrick:

$$n\,Cl-R-Cl + n\,Na_2S_x \rightarrow (-R-S_x-)_n + 2n\,NaCl$$
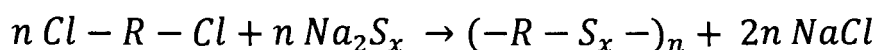
where alkyl chlorides, such as $(ClCH_2CH_2O)_2CH_2$, $ClCH_2CH_2Cl$, and $ClCH_2CH(Cl)CH_2Cl$, are used.[34] The energy of rotation of -S-S- links in the polysulfides' backbones is much less than the energy of rotation of -C-C- (3.9-4.4 Kcal/mol -C-C- vs. 0.95-1.05 Kcal/mol -S-S-), which determines the polysulfides' superior flexibility and pliability.[35] Commercial polysulfide polymers are available in three forms: millable grades solid elastomers, water dispersions of high molecular weight polymer and liquid polymers. By modifying the end mercaptan groups and backbone structures, new properties can be introduced.

Sulfur is the distinguishing feature of the polysulfide polymers. This helps provide the polymers significant chemical resistance. The hydrocarboxy groups give the structure good flexibility and the absence of tertiary carbon increases UV stability.[36] Polysulfides are generally resistant to weathering.

However, likely due to their powerful unpleasant odor and environmentally unfriendly production technology, the use of polysulfides has declined eventually resulting in dramatic shrinkage of the research and the market on polysulfides after the 1980's. The development of other synthetic elastomers, such as silicones and polyurethanes, has made the shrinkage even worse. Polysulfides mainly used as coatings, sealants, and adhesives account for about 167 million dollars of the total 1111 million dollars of the U. S. sealant market according to 1995's sales data.[32] The brand of Thiokol® has been transferred from its founder, Thiokol Chemical Corporation, to Morton International in 1969, then to Rohm and Haas in 1999. In the spring of 2001, Rohm and Hans announced to exit the polysulfide market, which left the world polysulfide supply with a huge void.[37] Today, the demands of polysulfides in North America have been fulfilled by Toray Industries, Inc. (Japan), and

Chemiewerke (Germany) also produces a polysulfide polymer. PRC-Desoto and Diamond Shamrock Corporation also produce other mercaptan terminated polymers.

2.4. References

1.   U. R. Evans, J. E. O. Mayne, Protection by paints richly pigmented with Zn dust. *Society of Chemical Industry Journal* **1944,** *22*, 109-110.

2.   S. Feliu, R. Barajas, J. M. Bastidas, M. Morcillo, Mechanism of cathodic protection of zinc-rich paints by electrochemical impedance spectroscopy. I. Galvanic stage. *Journal of Coatings Technology* **1989,** *61* (775), 63-69.

3.   S. Feliu, R. Barajas, J. M. Bastidas, M. Morcillo, Mechanism of cathodic protection of zinc-rich paints by electrochemical impedance spectroscopy. II. Barrier stage. *Journal of Coating Technology* **1989,** *61* (775), 71-76.

4.   R. A. Armas, C. A. Gervasi, A. Di Sarli, S. G. Real, J. R. Vilche, Zinc-rich paints on steels in artificial seawater by electrochemical impedance spectroscopy. *Corrosion* **1992,** *48* (5), 379-383.

5.   H. Marchebois, S. Joiret, C. Savall, J. Bernard, S. Touzain, Characterization of zinc-rich powder coatings by EIS and Raman spectroscopy. *Surface and Coatings Technology* **2002,** *157* (2-3), 151-161.

6.   Z. W. Wicks Jr., F. N. Jones, S. P. Pappas, D. A. Wicks, *Organic Coatings: Science and Technology, 3rd edition.* Wiley-Interscience: Hoboken, NJ, 2006.

7.   D. Pereira, J. D. Scantlebury, M. G. S. Ferreira, M. E. Almeida, The application of electrochemical measurements to the study and behaviour of zinc-rich coatings. *Corrosion Science* **1990**, *30* (11), 1135-1147.

8.   J. R. Vilche, E. C. Bucharsky, C. A. Giúdice, Application of EIS and SEM to evaluate the influence of pigment shape and content in ZRP formulations on the corrosion prevention of naval steel. *Corrosion Science* **2002**, *44* (6), 1287-1309.

9.   G. P. Bierwagen, CPVC Calculations. *Journal of Paint Technology* **1972**, *44* (46), 574.

10.   G. P. Bierwagen, A Re-Examination of the CPVC as a Transition Point in Coatings Behavior. *Journal of Coating Technology* **1992**, *64*, 71-75.

11.   W. K. Asbeck, A Critical Look at CPVC Performance and Applications Properties. *Journal of Coating Technology* **1992**, *64*, 47-58.

12.   N. Birbilis, R. G. Buchheit, Electrochemical Characteristics of Intermetallic Phases in Aluminum Alloys. *Journal of the Electrochemical Society* **2005**, *152* (4), B140-B151.

13.   D. Battocchi, A. M. Simões, D. E. Tallman, G. P. Bierwagen, Electrochemical Behavior of a Mg-rich Primer in the Protection of Al alloys. *Corrosion Science* **2006**, (48), 1292-1306.

14.   P. C. Grevatt, Toxicological Review of Hexavalent Chromium. EPA, U., Ed. Washington, DC, August 1998.

15.   M. E. Nanna, G. P. Bierwagen, Mg-Rich Coatings: A New Paradigm for Cr-Free Corrosion Protection of Al Aerospace Alloys. *Journal of Coating Technology Research* **2004**, (1), 69-81.

16.   G. P. Bierwagen, D. Battocchi, A. Simões, A. Stamness, D. Tallman, The use of multiple electrochemical techniques to characterize Mg-rich primer for Al alloys. *Progress in Organic Coatings* **2007,** (59), 172-178.

17.   J. Li, J. He, B. J. Chisholm, D. Battocchi, G. P. Bierwagen The development of a two-component, magnesium-rich primer for controlling corrosion of aluminum alloys. *Proceeding of 34th International Waterborne, High-Solids, and Powder Coatings Symposium* **2007,** 115-130.

18.   D. Battocchi, G. P. Bierwagen, A. Stamness, D. Tallman, A. Simões, Magnesium-rich primers for chromate-free protective systems on Al 2024 and Al 7075. L. Fedrizzi, H. T., A. Simões, Ed. Woodhead Publishing, Ltd: Cambridge, UK, 2007; pp 63-71.

19.   A. Simões, D. Battocchi, D. Tallman, G. P. Bierwagen, Assessment of the Corrosion Protection of Aluminium Substrate by a Mg-Rich Primer: EIS, SVET snf SECM Study. *Journal of Electrochemistry Society* **2008,** *155*, E143-E149.

20.   H. Xu, D. Battocchi, D. E. Tallman, G. P. Bierwagen, Use of Mg Alloys as Pigments in Mg-rich Primers for Protection Al Alloys. *Corrosion* **2009,** *65*, 318-325.

21.   A. M. Simões, D. Battocchi, D. Tallman, G. P. Bierwagen, SVET and SECM Imaging of Cathodic Protection of Aluminium by a Mg-rich Coating. *Corrosion Science* **2007,** *49*, 3838-3849.

22.   E. A. Grulke, *Polymer Process Engineering*. PRT Prentice Hall: Englewood Cliffs, NJ, 1994.

23.   J. M. G. Cowie, V. Arrighi, *Polymers: Chemistry and Physics of Modern Materials (3rd edition)*. CRC Press: Boca Raton, FL, 2008.

24. A. Blaga, Properties and Behaviour of Plastics. http://www.nrc-cnrc.gc.ca/eng/ibp/irc/cbd/building-digest-157.html.

25. Z. W. Wicks Jr., F. N. Jones, S. P. Pappas, D. A. Wicks, *Organic Coatings: Science and Technology, 3rd edition*. Wiley-Interscience: Hoboken, NJ, 2007.

26. T. A. Osswald, G. Menges, *Materials Science of Polymers for Engineers*. Hanser: Cincinnati, 1995.

27. J. Mark, B. Erman, *Science and Technology of Rubber, 3rd edition*. Elsevier Academic Press: London, 2005.

28. J. C. Patrick, N. M. MNookin Vulcanizable Compounds and Volcanized Products Derived Therefrom. 1,890,231, 1932.

29. S. K. Flanders, R. C. Klingender, Polysulfide Elastomers. In *Handbook of Specialty Elastomers*, Robert C. Klingender, K. C. K., Ed. 2007; pp 371-385.

30. N. Akmal, A. M. Usmani, Polysulfide Sealants and Adhesives. In *Handbook of Adhesive Technology, Second Edition*, Mittal, A. P. a. K. L., Ed. 2003; pp 531-539.

31. J. S. Amstock, Polysulfide and LP Polymers. In *Handbook of Adhesives and Sealants In Construction*, McGraw-Hill: New York, 2001.

32. T. C. P. Lee, *Properties and Applications of Elastomeric Polysulfides*; 1999.

33. J. R. Panek, Polysulfide Sealants and Adhesives. In *Handbook of Adhesives, 3rd edition*, Skiest, I., Ed. van Nostrand Reinhold: New York, 1992.

34. E. A. Peterson, Polysulfides. In *Engineered Materials Handbook*, AMS International: 1990; Vol. Adhesives and Sealants, 3.

35. T. Tsareva, L. Rappoport Method of Synthesis of N-acetyl Substituted Urethane Polymers. 1979.

16

36. The Adhesive and Sealant Council, Inc. (ASC) Joint Sealants. http://www.wbdg.org/design/079200.php.

37. Rohm and Haas to Exit Liquid Polysulfide Business. http://www.adhesivesmag.com/Articles/Industry_News/fead602907ac8010VgnVCM10000 0f932a8c0_____.

CHAPTER 3. CHARACTERIZATION METHODS

3.1. Abstract

An introduction to the electrochemical and mechanical characterization methods which was utilized in this research of the sulfur-based Mg-rich primer is given in this chapter, which includes Electrochemical Impedance Spectroscopy (EIS), Electrochemical Noise Measurement (ENM), accelerated weathering methods, Dynamic Mechanical Thermal Analysis (DMTA), Nano-indentation Technique, and a variety of empirical tests usually used to test aerospace coatings.

3.2. Electrochemical Impedance Spectroscopy (EIS)

EIS is one of the most commonly used methods for evaluation of coating corrosion protective properties.[1-5] A three-electrode configuration is normally used for EIS tests in the data acquisition of coated objects (Figure 2). As shown in the figure, the metal substrate is connected to the working electrode lead (WE), and a platinum mesh used as the counter electrode (CE) and a reference electrode (RE), like the saturated calomel electrode (SCE) used in the following experiments, is immersed with the sample in the diluted Harrison's solution, an electrolyte extensively used in electrochemical research.[6] Some auxiliary devices are also needed: a grounded Faraday Cage completely surrounding the cell and all the electrodes to reduce current noise from environment, and a personal computer to collect and analyze data. A small-amplitude AC voltage signal with varying frequencies is applied

on the sample, and the responding AC current data of working electrode is collected. Thus, the generated impedance data obtained at low frequency is frequently used in the EIS data analysis as it is comparable to the polarization resistance of coated metals and can be related to the barrier protection performance of the coating.

However, when the three-electrode configuration is not feasible or cannot be applied, a two-electrode configuration will generally be used.[7-13] In such cases, a piece of noble metal (usually gold) is deposited onto the coating surface and used as both the reference and counter electrode.
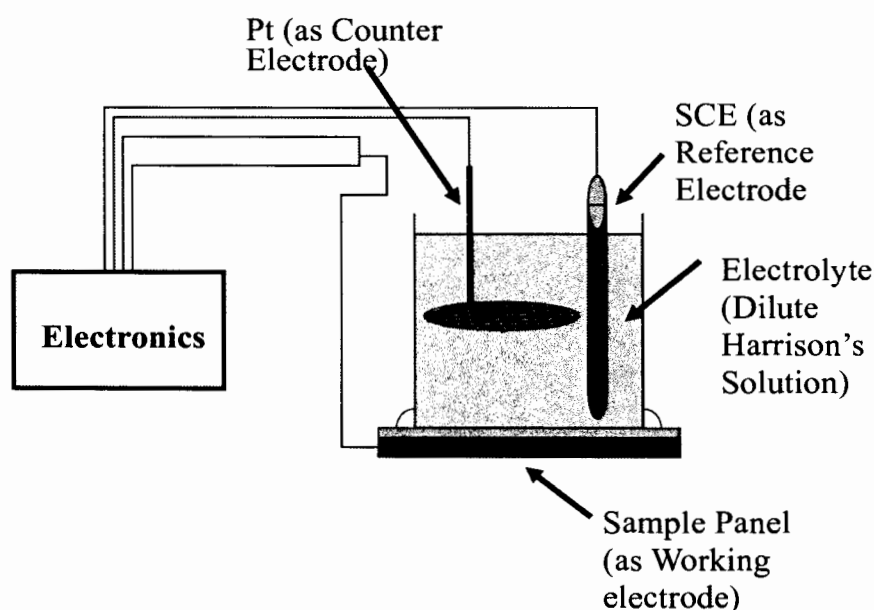

Figure 2. Setup of the three-electrode EIS method.

3.3. Electrochemical Noise Measurement (ENM)

Observation of electrochemical noise (ECN) in the corrosion process and electrochemical studies were first reported in the late 1960s and 1970s.[14-17] Nowadays,

19

ENM has been extensively used in the characterization of the corrosion protection property of coatings due to availability of digital equipment which makes the measurement and recording of noise data an easier task.[6, 18-20] Because this technique measures the electric noise fluctuations which originate from the tested samples and no outside electrical perturbation is applied during the test, it is absolutely non-intrusive and can be used for continuous monitoring of the corrosion protection performance of coatings. Thus, it is especially useful in studies of localized corrosion for the laboratory research and testing, or on-site troubleshooting and process control. Similar to some other electrochemical methods, ENM can give fast and quantitative evaluation of the coating performance. Electrochemical noise measurement involves monitoring two major types of electrochemical spontaneous fluctuations. One is potential noise, which is the fluctuation of the electrical potential between a working electrode and a reference electrode. The other is current noise, which is the fluctuation of the electric current at one electrode or between two working electrodes.[21] Both the potential noise and the current noise need to be measured simultaneously when the corrosion protection performance of a coating is studied.

Current and potential fluctuations of corroding systems are currently measured mainly using the cell arrangement with two working electrodes proposed by Eden et al.[22, 23] This approach was first proposed in the early 1980s by Hladky and Dawson.[24] The electrochemical noise measurement is normally carried out between two identical coated panels (Figure 3). A cell is attached onto each panel and it is filled with aqueous electrolyte. A salt bridge is used for the electrical connection of the electrolyte in two cells. A reference electrode is placed in one cell. The two working electrode leads are connected to the metal substrates. The potential noise is measured between the reference electrode and the metal

substrate, while the current noise is measured between the two working electrodes by a zero resistant ammeter (ZRA) that allows very small current measurement to be obtained without disturbing the corrosion cell circuit.
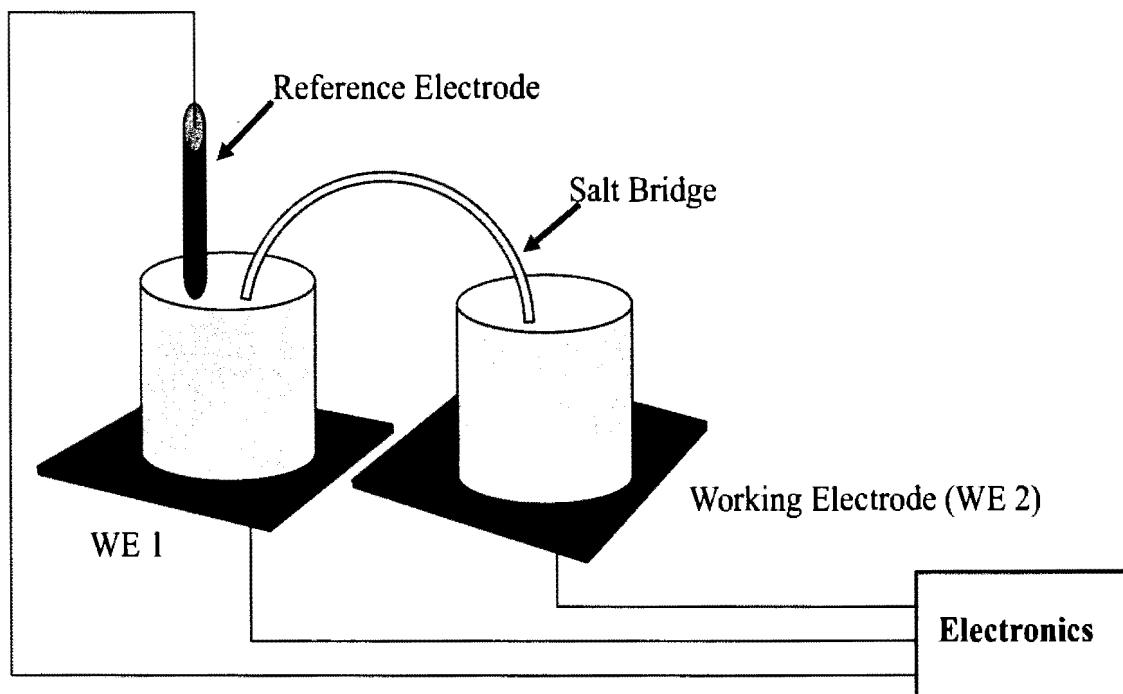
Figure 3. Setup of electrochemical noise measurement.

3.4. Accelerated Weathering Methods

The purpose of coating weathering is to predict if the exterior durability of a given coating can satisfy the service life demanded. However, it usually takes months or years to find out the results if the coating is weathered at the service condition. Some specific locations are chosen for accelerated outdoor exposure testing. Southern Florida has a subtropical climate with high humidity, high annual rainfall, high temperature, and high

intensity sunlight. Arizona has more annual sunshine hours, a higher average daily high temperature, and greater temperature fluctuations, but low humidity. These unique climates are especially useful for testing certain types of coatings, like the outdoor weathering site in Arizona which is particularly effective in causing changes in color and gloss of coatings, as well as heat aging and physical properties.[25, 26] In addition, various exposure techniques are used at such locations to simulate other service conditions and to accelerate corrosion processes, such as salt water spray for predicting long term corrosion protection of coated panels, black box for imitating the condition found on the trunk and hood of an automobile, etc.[26]

In reality, not all experiments can be carried out at such locations. Thus, artificial laboratory accelerated weathering devices were created in order to provide laboratory tools for developing new coating formulations. The natural exposure environment parameters, such as temperature, the intensity of UV radiation, humidity and the concentrations of corrosive reagents, are simulated in the accelerated weathering devices, but the stress levels need to be carefully set so that, on one hand, the more intense stress can achieve an more accelerated aging of the coating under examination, and on the other hand, the artificial acceleration can lead to an degradation process which emulates accurately as those known to occur under service conditions.[27, 28]

Not only can the lifetime of the coating system be predicted by using accelerated weathering testing, but also the users can study and rank the coating's performance by measuring changes of chemical and mechanical properties during testing. The parameters considered include gloss, color, contact angle/surface energy, electrochemical

investigations for corrosion protective systems, topography, chemical structure, and so on.[29, 30] These measurements are usually done at a regular interval, such as every week.

Many standardized laboratory accelerated weathering devices are available for accomplishing salt spray chamber exposure, cyclic salt chamber exposure, UV weathering, thermal cycling exposure, etc. Although these methods are widely used, results obtained from any single method usually do not correlate directly with those from actual field exposure. The lack of correspondence between the results from real exposure conditions may occur because artificial accelerated weathering devices are subjected to the simplified environmental stress level sets: if only a few stresses are taken into consideration, one cannot guarantee an equivalence of results due to possible unknown causes. [28, 31]

In this research, two accelerated weathering exposure protocols, ASTM B 117 (Standard Practice for Operating Salt Spray (Fog) Apparatus) and ASTM D 5894 (Standard Practice for Cyclic Salt/Fog UV Exposure of Painted Metal, shown in Figure 4,) were used separately. ASTM B 117 provides a controlled corrosive environment representing accelerated marine type atmospheric conditions. Correlation of test results to in-service (field) performance should only be considered if supported by results from long term in-service atmospheric exposures. It has been recognized for many years now that little correlation exists between the results from salt-spray tests and in-service performance. ASTM D 5894 is generally regarded as giving a better correlation with outdoor exposure results, and is a sequential Prohesion/QUV accelerated weathering test. At present, D 5894 is the best general accelerated test method for coating systems intended for atmospheric exposure.[30]
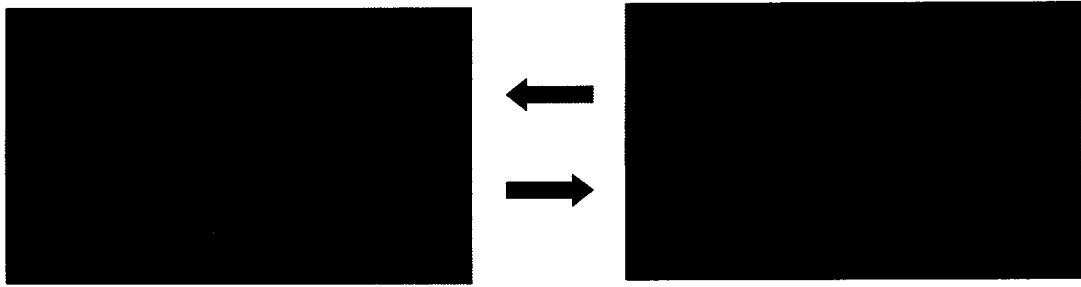
Figure 4. Flowchart of ASTM D5894 weathering protocol.

3.5. Dynamic Mechanical Thermal Analysis (DMTA)

Polymeric materials have a special behavior that many materials, such as metals, do not. As viscoelastic materials, they have both solid and liquid properties. One of the most powerful methods used to investigate the viscoelastic properties of polymeric materials is Dynamic Mechanical Thermal Analysis (DMTA). DMTA can measure dynamic mechanical properties, as well as tensile properties. Theory and measurement of tensile properties has been discussed in the previous chapter. The measurement of dynamic mechanical properties will be discussed below.

In order to measure dynamic mechanical properties, like storage modulus and loss modulus, the DMTA technique uses a very small sinusoidally varying stress to a test piece at a constant frequency as the temperature is increased at a constant rate. The strain is recorded and three dynamic mechanical parameters can be calculated: the storage modulus (E', with stress and strain in phase), the loss modulus (E'', with stress and strain out of phase), and the loss factor (tan δ) that is the phase angle between the stress and the strain. These can be described in terms of angular frequency ω:

$$E(\omega) = E'(\omega) + iE''(\omega)$$.......................Equation 4

24

$$\tan \delta = \frac{E''(\omega)}{E'(\omega)} \dots\dots\dots\dots\dots\dots\dots\dots\dots\text{Equation 5}$$

where $E(\omega)$ is the frequency-dependent complex dynamic modulus, of which the real part $E'(\omega)$ and the imaginary part $E''(\omega)$ are called storage modulus and loss modulus respectively.[32]

Determination of dynamic mechanical and tensile properties requires the use of free film. This requirement is a serious limitation to coating films because the influence on the coating from the substrate cannot be reflected.

3.6. Empirical Tests of Aircraft Coatings

A number of factors affect the performance of aircraft coatings, including the aircraft's operational environment and the coating's durability. Therefore, selection of appropriate test and evaluation procedures is an essential component for determining acceptable coatings for aircraft application.

3.6.1. Conical Mandrel Bending Experiments

DMTA for the flexibility measurement has been discussed. Both the conical mandrel bending tests and the impact resistance tests are often used for evaluating the flexibility of coatings in the coating laboratory.

The conical mandrel bending test requires a manual bending of a coated flexible metal panel over a cone. As described in ASTM D 522 (Test Method for Elongation of Attached Organic Coatings with Conical Mandrel Apparatus), testing items include a

conical mandrel tester and coated 0.8 mm-thick cold-rolled steel panels. The crack
resistance value is obtained by measuring the length of the crack occurring on the coating,
and the length of the crack can be converted to percent elongation from a plot given in
ASTM D 522 (shown in Figure 5).

3.6.2. Impact Resistance Experiments

The impact tester drops a heavy indenter through a guiding tube on a coated panel
resting on a platform. A die in the platform allows the panel to be pushed down by the
indenter to form a crater in the panel. Cracking observed around the impact-produced crater
is considered as failure, and weight and height is recorded in inch-pounds. ASTM D 2794
(Test Method for Resistance of Organic Coatings to the Effects of Rapid Deformation)
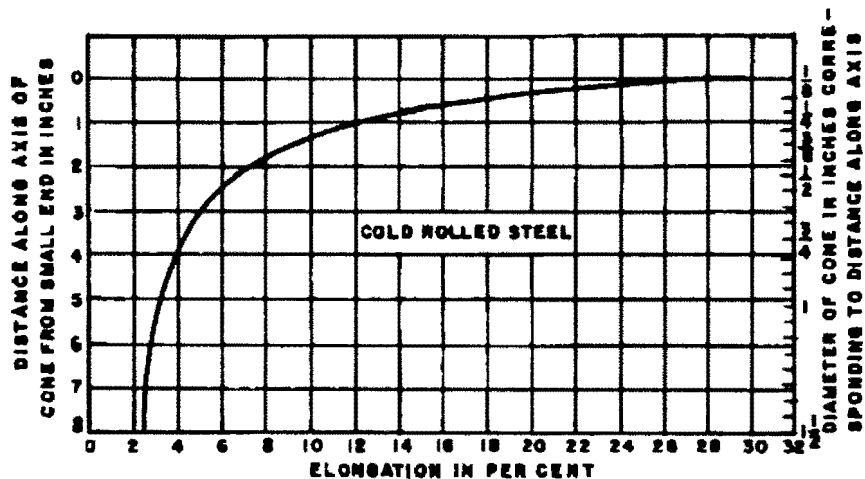describes such a test procedure.

Figure 5. Distance along cone and corresponding mandrel size versus percent elongation
for specimens on cold-rolled steel 0.8mm in thickness.[33]

26

3.6.3. Organic Solvent Resistance Experiments (MEK Double Rubs)

Resistance to organic solvents is usually performed by rubbing a coated panel with a cheese cloth soaked with an organic solvent, usually MEK. After rubbing, the coating is inspected for color change, dissolution, or any abnormal change caused by the solvent. ASTM D 4752 (Standard Test Method for Measuring MEK Resistance of Ethyl Silicate (Inorganic) Zinc-Rich Primers by Solvent Rub) and ASTM D 5402 (Standard Practice for Assessing the Solvent Resistance of Organic Coatings Using Solvent Rubs) can be referred to when the experiments are taken.

3.7. Nano-Indentation Technique

The nanoindentation technique was developed in recent decades to study the microtribology of solid materials. The main component of a nanoindentation instrument is a transducer that can transfer mechanical signals obtained from the probe into electrical signals to be processed by a data acquisition system. The signal inputs are then output with the load/displacement curves. Local hardness and reduced modulus of the tested materials are then collected carrying out the fitting to the load/displacement curves. The equations of hardness (H) and reduced modulus (E_r) are given below:

$$H = \frac{F_{max}}{A} \quad\ldots\ldots\ldots\ldots\ldots\ldots\ldots\ldots\ldots\ldots\ldots\ldots \quad \text{Equation 6}$$

$$\frac{1}{E_r} = \left(\frac{1-\upsilon^2}{E}\right)_{sample} + \left(\frac{1-\upsilon^2}{E}\right)_{indenter} \quad\ldots\ldots\ldots\ldots\ldots \quad \text{Equation 7}$$

where F_{max} is the maximum load; A is the contact area between the probe and the sample; v is the Poisson ratio; E is the elastic modulus. The probe is made of diamond, and for a diamond indenter, $E_{indenter}$ is 1140GPa and Poisson's ratio is 0.07, while for most materials, Poisson's ratio is around 0.4. Thus the expression of reduced modulus can be written as:

$$E_r \approx E_{sample} \text{ ⁇} \dots\dots\dots\dots\dots\dots\dots\dots\dots\dots \text{ Equation 8}$$

The contact area A, also called projected area, can be determined according to different cases by using light microscopy. But when the light microscopy is not available, to determine the area function, a series of indents at a variety of contact depths are made on a fused quart whose elastic modulus is known, and the contact area A is calculated. For the probe tips of different shapes, the expression of the contact area could be different. For an ideal Berkovich probe, A can be written as:[34, 35]

$$A = 24.5{h_c}^2 \dots\dots\dots\dots\dots\dots\dots\dots\dots\dots\text{Equation 9}$$

where h_c is the contact depth. The relationship of the parameters is illustrated in the following figure:

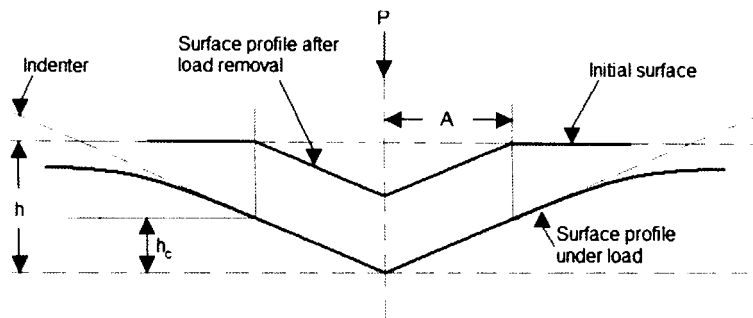Figure 6. Schematic of indentation.[34]

3.8. References

1. G. P. Bierwagen, D. Tallman, J. Li, L. He, C. Jeffcoate, EIS studies of coated metals in accelerated exposure. *Progress in Organic Coatings* **2003,** *46* (2), 148-157.

2. G. P. Bierwagen, L. He, J. Li, L. Ellingson, D. E. Tallman, Studies of a new accelerated evaluation method for coating corrosion resistance — thermal cycling testing. *Progress in Organic Coatings* **2000,** *39* (1), 67.

3. J. N. Murray, Electrochemical test methods for evaluating organic coatings on metals: an update. Part III: Multiple test parameter measurements. *Progress in Organic Coatings* **1997,** *31* (4), 375-391.

4. A. Amirudin, D. Thieny, Application of electrochemical impedance spectroscopy to study the degradation of polymer-coated metals. *Progress in Organic Coatings* **1995,** *26* (1), 1-28.

5. J. A. Grandle, S. R. Tayler, Electrochemical Impedance Spectroscopy as a Method to Evaluate Coated Aluminum Beverage Containers: I. Determination of an Optimal EIS Parameter for Large Sample Evaluation. *Corrosion* **1994,** *50* (10), 792-803.

6. R. Cottis, S. Turgoose, *Electrochemical Impedance and Noise*. NACE International: Houston, TX, **1999**.

7. G. D. Davis, C. M. Dacres, M. B. Shook, Development of an Electrochemistry-based Corrosion Sensor to Monitor Corrosion of Boiler Tubes, Pipes, and Painted Structures. In *Proceeding of SPIE - Int. Soc. Optical Eng.*, Society of Photo-Optical Instrumentation Engineers, Bellingham, WA, INTERNATIONAL: **1998**; pp 92-101.

8.   T. C. Simpson, P. J. Moran, W. C. Moshier, G. D. Davis, B. A. Shaw, C. O. Arah, K. L. Zankel, An Electrochemical Moniter for the Detection of Coating Degradation in Atomsphere. *Journal of the Electrochemistry Society* **1989**, *136*, 2761-2762.

9.   T. C. Simpson, P. J. Moran, H. Hampel, G. D. Davis, B. A. Shaw, C. O. Arah, T. L. Fritz, K. L. Zankel, Eletrcochemical Monitoring of Organic Coating Degradation During Atomspheric or Vapor Phase Exposure. *Corrosion* **1990**, *46*, 331-336.

10.   T. C. Simpson, H. Hampel, G. D. Davis, C. O. Arah, T. L. Fritz, P. J. Moran, B. A. Shaw, K. L. Zankel, Evaluation of the Effects of Acidic Deposition on Coated Steel Substrates. *Progress in Organic Coatings* **1992**, *20*, 199-216.

11.   G. D. Davis, C. M. Dacres, L. A. Krebs Adhesive Tape Sensor for Detecting and Evaluating Coating and Substrate Degradation Utilizing Electrochemical Processes. **2001**.

12.   G. D. Davis, C. M. Dacres, Electrochemical Sensors for Evaluating Corrosion and Adhesion on Painted Metal Structures. **1999**.

13.   G. D. Davis, C. M. Dacres Portable, Hand-held, in-situ Electrochemical Sensor for Evaluating Corrosion and Adhesion on Coated or Uncoated Metal Structures. **2000**.

14.   W. P. Iveson, Transient Voltage Changes Produced in Corroding Metals and Alloys. *Journal of Electrochemistry Society* **1968**, *115*, 617-618.

15.   V. A. Tyagai, N. B. Lukyanchikova, Electrochemical noise of iodine reduction on a cadmium sulfide surface. *Sueface Science* **1968**, *12*, 331-340.

16.   V. A. Tyagai, N. B. Lukyanchikova, Electrochemical noise of reversible electrode reactions *Electrochimica Acta* **1973**, *18*, 229-230.

17.   V. A. Tyagai, Faradaic noise of complex electrochemical reactions. *Electrochimica Acta* **1971**, *16*, 1647-1654.

18.   G. P. Bierwagen, V. Balbyshev, D. Mills, D. Tallman In *Fundamental Considerations on Electrochemical Noise Methods to Examine Corrosion under Organic Coatings*, Proceeding of the Symposium on Advances in Corrosion Protection by Organic Coatings II, D.Scantlebur, M. K., Ed. Special Publication of The Electrochemical Society: **1995**; pp 69-81.

19.   G. P. Bierwagen, C. J. Jeffcpate, J. Li, S. Balbyshev, D. E. Tallman, The Use of Electrochemical Noise Methods to Study Thick, High Impedance Coatings. *Progress in Organic Coatings* **1996**, *29*, 21-30.

20.   G. P. Bierwagen, D. J. Mills, D. E.Tallman, and B. S.Skerry, Reproducibility Analysis of Electrochemical Noise Data For Coated Metal Systems. In *Electrochemical Noise Measurement for Corrosion Applications*, J.L.Kearns, J. R. S., P.R.Roberge, D.L.Reichert, Ed. ASTM Special Technical Publication: Philadelphia, **1996**; pp 427-445.

21.   D. A. Eden, *Uhlig's Corrosion Handbook, 2nd Edition*. John Wiley & Sons: Hoboken, NJ, **2000**.

22.   B. S. Skerry, Eden, D. A., Electrochemical testing to assess corrosion protective coatings. *Progress in Organic Coatings* **1987**, *15* (3), 269-285.

23.   D. A. Eden, M. Hoffman, B. S. Skerry, *Application of Electrochemical Noise Measurement to Coated Systems*. Washington D.C., **1986**; p 36.

24.   K. Hladky, J. L. Dawson, The measurement of localized corrosion using electrochemical noise. *Corrosion Science* **1981**, *21* (4), 317-322.

25.   J. E. Pickett, M. M. Gardner, Reproducibility of Florida weathering data. *Polymer Degradation and Stability* **2005**, *90* (3), 418-430.

26.   L. F. E. Jacques, Accelerated and outdoor/natural exposure testing of coatings. *Progress in Polymer Science* **2000,** *25* (9), 1337-1362.

27.   F. Deflorian, S. Rossi, L. Fedrizzi, C. Zanella, Comparison of Organic Coating Accelerated Tests and Natural Weathering Considering Meteorological Data. *Progress in Organic Coatings* **2007,** *59*, 244-250.

28.   U. Schulz, P. Trubiroha, U. Schernau, H. Baumgart, The effects of acid rain on the appearance of automotive paint systems studied outdoors and in a new artificial weathering test. *Progress in Organic Coatings* **2000,** *40*, 151-165.

29.   R. Baboian, *Corrosion Tests and Standards.* ASTM: Philadelphia, **1995.**

30.   G. P. Bierwagen, D. E. Tallman, Choice and Measurement of Crucial Aircraft Coatings System Properties. *Progress in Organic Coatings* **2001,** *41* (4), 201-216.

31.   K. M. Wernståhl, Service life prediction of automotive coatings, correlating infrared measurements and gloss retention. *Polymer Degradation and Stability* **1996,** *54* (1), 57-65.

32.   J. M. G. Cowie, V. Arrighi, *Polymers: Chemistry and Physics of Modern Materials (3rd edition).* CRC Press: Boca Raton, FL, **2008.**

33.   ASTM D522-93A, Standard Test Methods for Mandrel Bend Test of Attached Organic Coatings. **2001.**

34.   M. R. VanLandingham, J. S. Villarrubia, W. F. Guthrie, G. F. Meyers, Nanoindentaion of Polymers: An Overview. *Macromolecule Symposium* **2001,** *167*, 15-43.

35.   A. C. Tavares, J. V. Gulmine, C. M. Lepienski, L. Akcelrud, The effect of accelerated aging on the surface mechanical properties of polyethylene. *Polymer Degradation and Stability* **2003,** *81*, 367-373.

CHAPTER 4. RESULTS AND DISCUSSION OF ELECTROCHEMICAL MEASUREMENTS

4.1. Abstract

The flexible Mg-rich coatings were prepared with three different PVCs (30%, 40% and 45%), and exposed under two parallel laboratory accelerated weathering protocols with an advanced Mg-rich primer as a comparable group. Electrochemical corrosion measurements and visual inspection were used to monitor the process. The open circuit potential and impedance data were acquired to evaluate the corrosion protection performance of the Mg-rich primers. The 45% PVC flexible Mg-rich primer was found to provide the best corrosion protection among all the sulfur-containing Mg-rich coatings, and have a comparable performance as the standard Mg-rich primer.

4.2. Introduction

Hexavalent chromium, or chromate, as the current method to protect aluminum alloys against the threat of moisture, oxygen and other corrosive factors in the atmosphere, has been proven to be an effective and durable way to inhibit corrosion of aluminum alloys. However, due to the stricter regulations on the usage and disposal of chromates and other chromium containing compounds already established by regulators like the Environment Protection Agency (EPA), people have had to consider alternatives to chromate for protecting aluminum alloys.[1] The urgent need to replace toxic chromate-based primers leads to the development of magnesium rich primer as an alternative, which takes

33

magnesium particles mixed in organic or inorganic primers as the sacrifice anode to provide cathodic protection to aluminum alloys.[2-5] The application of sacrificial metal pigments in corrosion protection primers can be traced back to almost a half century ago when zinc rich primers (ZRPs) were put into the role of steel surface corrosion protection.[6] The mechanism by which the ZRP protects the steel substrate is primarily considered to be cathodic protection, and electrochemical properties of ZRPs have been extensively studied.[7, 8]

Similar with ZRP's mechanism, there has to be a galvanic contact between the aluminum substrate and magnesium particles in cured magnesium rich primers, as well as between magnesium particles. This means that the pigment volume concentration (PVC) must be higher than the critical pigment volume concentration (CPVC). With these electrical contacts, the substrate is polarized and the pigment/substrate mixed potential is known as open circuit potential (OCP), which can be measured by electrochemical methods. As the sacrificial particles are consumed and the electrical contacts are gradually lost, the barrier property of the mixture of binder and corrosion products of particle metal can still keep substrate from corrosion for a longer lifetime.[9] The barrier property can also be characterized by electrochemical impedance. [10]

In this chapter, to examine whether the flexible polysulfide binder can maintain, or even enhance, the corrosion protection property of Mg-rich primer, the electrochemical characterization of topcoated Mg-rich polysulfide flexible primer is examined in association with the visual appearance of testing panels during artificial accelerated weathering. The electrochemical characterization includes EIS and ENM methods, as described in Chapter 3. Comparisons of testing results are made between the newly

developed polysulfide-based Mg-rich primer and the newly commercialized epoxy-based Mg-rich primer XP417-183 under different artificial weathering protocols.

4.3. Experiment

4.3.1. Sample Preparation

In this primer system, amine modified polysulfide polyester was used as a hardener for curing epoxy component, both of which were provided by Chevron Phillips Chemical Company, and identified as TZ-H 904 ("H" stands for Hardener) and TZ-R 904, respectively. As instructed by manufacturer, the 100%-solid two-component TZ 904 coating, which was originally developed for protecting steel substrate for the Army's stricter emission requirement, needs a specialized plural component spraying equipment that is not available at NDSU. Instead, xylene was used in our lab to dissolve the two components in order to get appropriate viscosity to apply by ordinary spray gun or draw-down bar.

To overcome the flexibility problem on the-state-of-the-art Mg-rich epoxy primer, Mg pigment was mixed into the TZ 904 coating that can be elongated over 32% without cracks. The practical equation to calculate the Pigment Volume Concentration (PVC) is given as:

$$PVC = (W_{Mg}/\rho_{Mg}+10\% \times W_R/\rho_R)/(W_R/\rho_R + W_H/\rho_H + W_{Mg}/\rho_{Mg}) \dots \dots \text{Equation 10}$$

where W_{Mg} is the weight of Mg, W_R is the weight of the resin TZ-R 904, and W_H is the weights of the hardener TZ-H 904. The density of Mg, ρ_{Mg}, is 1.74g/cm^3, the density of the resin, ρ_R, is 1.15g/cm^3, and the density of the hardener, ρ_H, is 0.965 g/cm^3. There are 10% TiO$_2$ fillers in volume pre-mixed in TZ-R 904, which is also counted for the pigment volume, and represented by $10\% \times W_R/\rho_R$ in the Equation 10.

The steps of primer preparation method are listed below:

1. Both of the components are separately dissolved in xylene (Sigma-Aldrich, 214736-4L) with weight ratio of 1:1 roughly. Hand-stirring is required considering the polymers are highly viscous and cannot be dissolved automatically.

2. After calculation by the Equation 10 above, an appropriate amount of Mg-3820 particles provided by Ecka-Granules of America (Louisville, KY), which are made of pure magnesium surrounded by magnesium oxide, is added into the dissolved epoxy. The mixture is first stirred by hand for 5 minutes and then ultrasonicated by Aquasonic® ultrasonic dispersion for one hour to obtain better dispersion.

3. The dissolved hardener is added into resin/pigment mixture as stirred by hand. Based on the information provided by Chevron Phillips Company, one volume part of hardener is required to cure one volume part of resin to get the best result.

4. When the Mg-rich primers are coated on metal substrates, they are left in a 70°C oven for a whole day to make sure that they are completely cured.

In order to improve the substrate surface's adhesion, aluminum alloy 2024-T3 panels were pretreated through the aluminum panel cleaning system newly established by

the United States Air Force. Then the primers were applied by ordinary spraying gun when the substrate surface was dry.
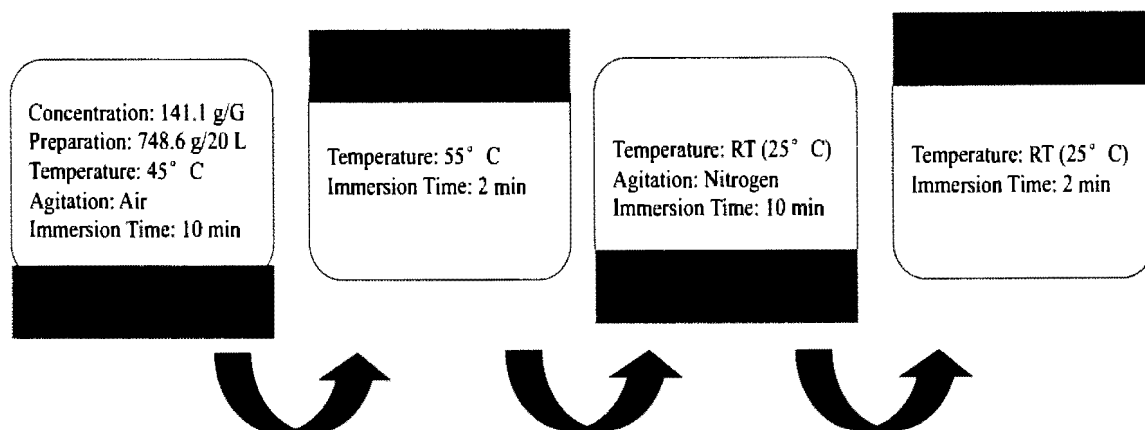

Figure 7. Flowchart of aluminum alloy panel pretreatment bath.

Aluminum panels of AA2024-T3 with dimensions of 3"×6", supplied by Q Panel Lab products (Cleveland, OH), were used in the tests. Coupons of bare aluminum alloy AA2024-T3 were cleaned in a standard four bath cleaning process shown as a flow chart in Figure 7. The first step is 10-min immersion in Oakite® Aluminum Cleaner 164 (alkaline detergent, Oakite Products, Detroit, MI) with moderate air agitation at 45°C. The second step is 2-min immersion in distilled water at 55 °C. The third step is 10-min room-temperature immersion in Turco SMUT-Go NC deoxidizer (Turco Products, Westminster, CA) with moderate nitrogen agitation. The final step is immersion in distilled water for 2 min at room temperature. To reduce bath contamination, the substrates were rinsed with distilled water briefly before the second and fourth steps.

The sulfur-containing Mg-rich primers were prepared with different PVCs: 30%, 40%, and 45%. The titanium dioxide particles already existing in TZ 904 make up 5% of

37

the PVCs and magnesium particles make up the rest. The commercial version of the Mg-rich primer XP417-183 supplied by Akzo-Nobel Aerospace Coatings Co. was used as the comparable coating. Each species was sprayed upon pretreated eight aluminum alloy AA2024-T3 panels with about 2 mil wet thickness. After the primers were cured, they were topcoated by a white glossy urethane topcoat 646-58-7925 from Akzo-Nobel, with a wet thickness of topcoat applied at 3-4 mils.

4.3.2. Artificial Weathering Protocols and Electrochemical Measurements

After painting, a uniform cross scribe was made down to the bare aluminum alloy substrate by Gravograph® rotating engraving machine on each panel. The backside and the edge of these panels then were covered with 3M® insulating tape and only the coatings with the cross scribe were kept exposed. The eight panels for each species were divided into two groups and placed in two artificial weathering protocols: ASTM B117 and ASTM D5894, briefly discussed in Chapter 3. These panels were electrochemically monitored and visual images of the coatings were recorded by a scanner after each week's exposure in the first 6 weeks (about 1000 hours), and the interval of measurements increases as the exposure time increases. The panels were taken out of the Prohesion chamber in the last ten minutes of the wet cycle exposure, or out of the QUV chamber in the last ten minutes of the first hour of the condensation cycle, to take ENM and EIS tests. Since ENM, rather than EIS, is a non-intrusive method to coatings' corrosion protection property measurement, it was always carried out before EIS when panels were taken out of artificial weathering chambers.

A schematic experimental setup for the ENM study is shown in Chapter 3. The electrochemical cell consisted of a glass cylinder reservoir which was clamped on the surface of coated panels through a rubber o-ring and filled with the electrolytic solution: dilute Harrison's solution (DHS). The DHS is used to emulate acid rain and consists of 0.35 wt.% $(NH_4)_2SO_4$ and 0.05 wt.% NaCl in distilled water. Each pair of the identical panels, from the same species and the same artificial weathering protocol, were connected by a NaCl agar salt bridge. Thus, this method is called the bridge method. The pairs of panels for noise measurement were fixed throughout the whole electrochemical study so that the noise data could be traceable and relatively stable. A saturated calomel electrode (SCE) was used as the reference electrode. The noise corresponding to response of both panels was monitored by a Gamry PC4/300 potentiostat/galvanostat with Gamry Framework software. 100-second initial delay was set to let the system reach open circuit potential. After the delay, time records of ZRA current and sample voltage were collected at 0.1 second sample time for a block time of 25.4 seconds in order to provide the standard deviation of the voltage and current, the ratio of which defines noise resistance R_n.

For EIS, of which the schematic experimental setup is also given in Chapter 3, a saturated calomel electrode (SCE) and a Platinum mesh with approximately 1 cm^2 area were used on a single coated panel as the reference electrode and the counter electrode, respectively. A Gamry PC4/300 potentiostat/galvanostat with Gamry Framework software was used to collect the electrochemical data associated with a multiplexer. Impedance spectra were recorded with a frequency sweep from 0.01 Hz to 100 kHz, and the amplitude of the signal perturbation was 10 mV.

4.4. Results and Discussion

4.4.1. Mg-rich Coatings' Corrosion Protection Performance

In order to simulate natural weathering conditions, two laboratory accelerated weathering protocols were deployed in the research to assess the Mg-rich coatings' corrosion protection behavior.

For ASTM B117 continuous salt spray protocol, a number of blisters were found along the scribe on the 30% and 40% PVC samples in a couple of weeks. But the size, as well as the number, of the blisters did not increase during the following weeks' exposure. Few blisters were observed on the 45% PVC Mg-rich coatings during the whole exposure period. At around the eighth week, white corrosion products appeared in the scribes made on both of the sulfur-based flexible Mg-rich coatings and commercialized Akzo Nobel aerospace Mg-rich coatings, and the amount of the corrosion products by visual observation was slowly increasing. The same situation can also be found on those lower PVC coatings. However, no delamination was observed on any sample which went through the instant salt spray protocol.

Prohesion/QUV alternating exposure is more destructive based on visual observation. White corrosion products and salts from Prohesion weathering chamber started to accumulate in the scribes since the sixth week, and completely covered the scribes at the 22nd week exposure except the 30% PVC sulfur based Mg-rich coating which failed earlier than that. The 30%, 40% and 45% PVC sulfur-containing Mg-rich coatings were found to be delaminated along the scribe at the 11th, 22nd, and 22nd week, respectively, while the Akzo Nobel aerospace Mg-rich coating was found delaminated at the 23rd week.

But during the whole Prohesion/QUV exposure process, there was no blisters forming along the scribes of any panels.
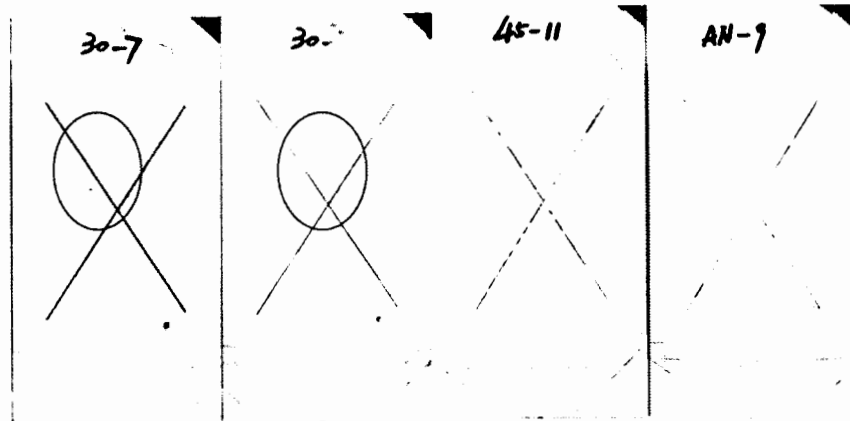

Figure 8. Images of panels from B117; from left to right: the 30% PVC flexible Mg-rich coating in the 1st week; the 30% PVC flexible Mg-rich coating in the 22nd week; the 45% PVC flexible Mg-rich coating in the 22nd week; the in flexible Mg-rich coating in the 22nd week. Pay attention to the blister in the red circles.
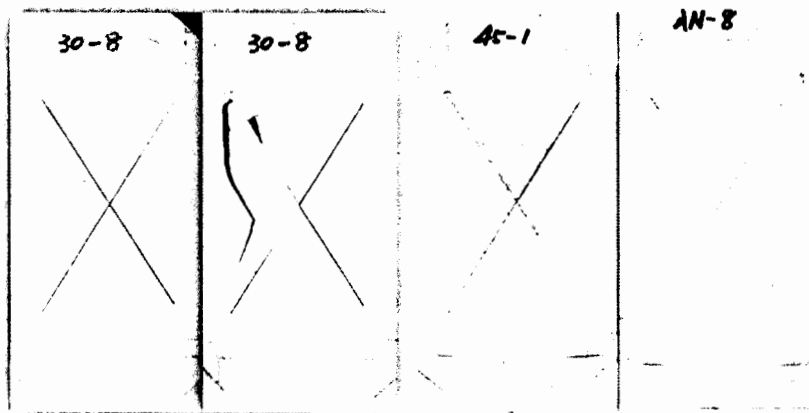

Figure 9. Images of panels from Prohesion/QUV; from left to right: the 30% PVC flexible Mg-rich coating in the 1st week; the 30% PVC flexible Mg-rich coating in the 11th week; the 45% PVC flexible Mg-rich coating in the 22nd week; the inflexible Mg-rich coating in the 22nd week.

4.4.2. Open Circuit Potential from Corrosion Potential Measurement

Open circuit potential (OCP or E_{oc}) achieved at the steady state is a very important parameter for monitoring the behavior of metal-rich coatings by measuring the potential of cathodically polarized substrate versus the reference electrode potential.[10, 11] Figure 10 illustrates the average OCP results obtained by corrosion potential measurement. The initial OCPs were around -1.0V ~ -1.4V, but increased dramatically in four weeks to -0.6 ~ -0.8V, and kept relatively stable until the end of exposure, which implies that Mg pigment particles were rapidly consumed in this four weeks, producing magnesium oxides precipitating. The results of the Akzo Nobel aerospace Mg-rich primer show the most cathodic OCPs, regardless of which weathering protocol they were obtained from. The samples, both sulfur based and epoxy based, from the B117 salt spray protocol have more negative OCPs than those from the Prohesion/QUV protocol, which are symbolized by solid spots and void spots respectively.

4.4.3. Impedance and Noise Resistance

The low frequency impedance modulus, Z_{mod}, can be used to predict the lifetime of the corrosion protection coatings and rank the performance of coatings' barrier property.[4, 9, 10, 12, 13] The results showing the average Z_{mod} at 0.01Hz frequency versus exposure time are given in Figure 11. The low frequency impedance moduli of samples from the B117 weathering method tends to decrease as the exposure time increases, while those from the Prohesion/QUV weathering protocol are relatively stable. Akzo Nobel aerospace Mg-rich primer has a better barrier property than other coatings based on its higher low frequency Z_{mod}.
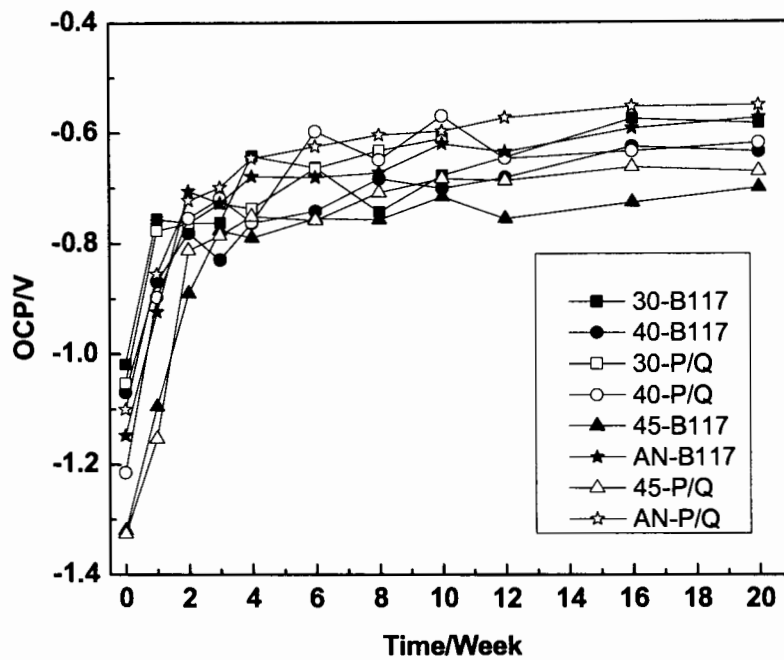
Figure 10. Open circuit potential vs. artificial weathering exposure time (P/Q means Prohesion/QUV weathering protocol).

Electrochemical noise measurements were also conducted at the coated samples and noise resistances (R_n) were obtained. Previous work showed that R_n is close to the polarization resistance and the low frequency Z_{mod}, and it is a good indicator of how much corrosion protection can be provided by the coatings.[14-17] Based on Figure 12, a similar conclusion can be drawn: Akzo Nobel aerospace Mg-rich primer has a better barrier property than the other coatings.
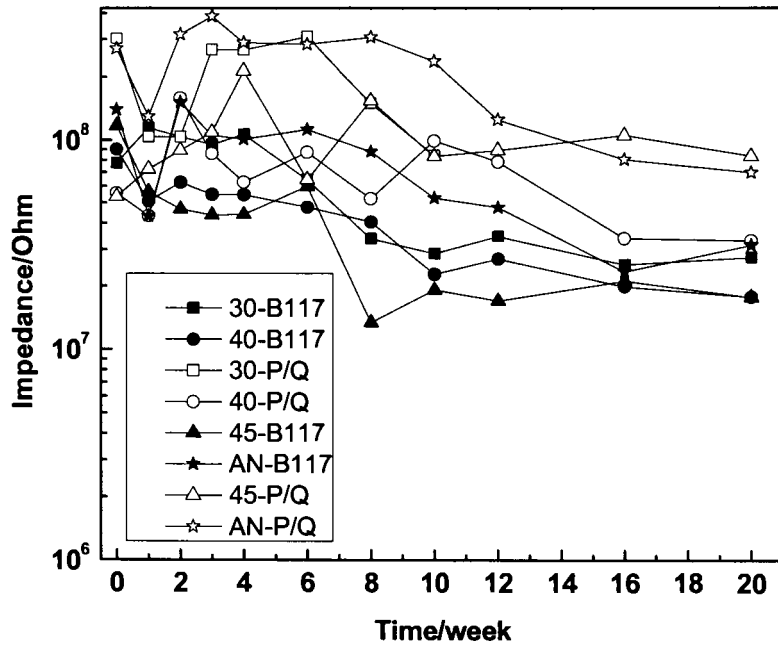
Figure 11. Z_{mod} at 0.01Hz changes according to weathering time increases.
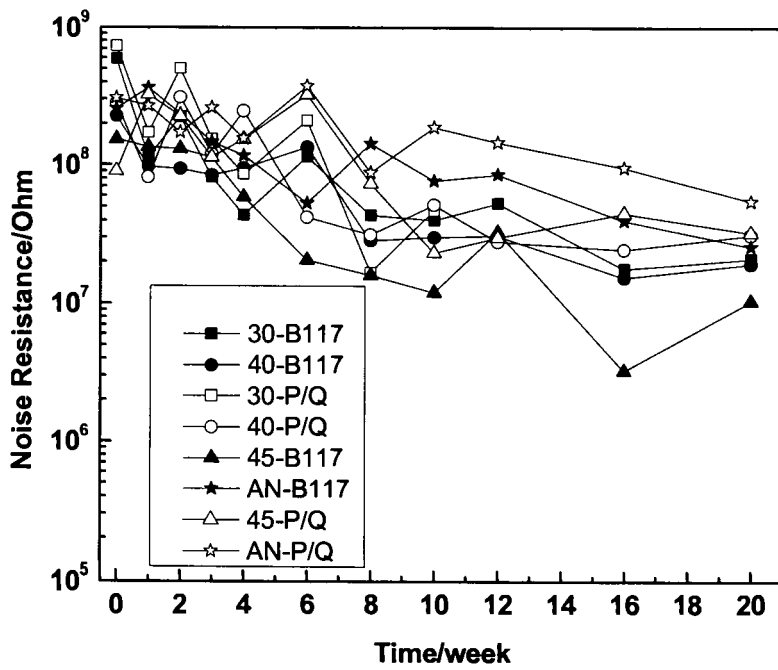

Figure 12. Noise resistance vs. artificial weathering time.

4.5. Conclusions

Two standardized laboratory accelerated weathering protocols, B117 and Prohesion/QUV alternating weathering, were deployed to simulate weathering conditions in an aggressive manner to induce accelerated coating failure. The samples were monitored by periodic visual checks combined with quantitative assessment using electrochemical methods: EIS and ENM. In this study, it was found that the Prohesion/QUV alternating weathering protocol is more aggressive than the B117 weathering method to Mg-rich coating systems. With a higher low frequency impedance, Akzo Nobel aerospace Mg-rich primer has better barrier property than the sulfur based Mg-rich primers. But the sulfur based Mg-rich primers can provide more cathodic protection during the exposure because of their more negative OCPs. It was found by visual comparisons that the corrosion protection property of Akzo Nobel Mg-rich coating is little, if any, better than the sulfur based Mg-rich coatings, which indeed contained less Mg pigment.

4.6. References

1.   P. C. Grevatt, Toxicological Review of Hexavalent Chromium. EPA, U., Ed. Washington, DC, August 1998.

2.   M. E. Nanna, G. P. Bierwagen, Mg-Rich Coatings: A New Paradigm for Cr-Free Corrosion Protection of Al Aerospace Alloys. *Journal of Coating Technology Research* **2004,** (1), 69-81.

3.   D. Battocchi, G. P. Bierwagen, A. Stamness, D. Tallman, A. Simões, Magnesium-rich primers for chromate-free protective systems on Al 2024 and Al 7075. L. Fedrizzi, H. T., A. Simões, Ed. Woodhead Publishing, Ltd: Cambridge, UK, 2007; pp 63-71.

4.   G. P. Bierwagen, D. Wang, K. Allahar, D. Battocchi, D. Tallman, Examination of Mg-rich coatings based on inorganic binders by EIS. *Electrochimica Acta, Submitted in June* **2007**.

5.   J. Li, J. He, B. J. Chisholm, D. Battocchi, G. P. Bierwagen The development of a two-component, magnesium-rich primer for controlling corrosion of aluminum alloys. *Proceeding of 34th International Waterborne, High-Solids, and Powder Coatings Symposium* **2007**, 115-130.

6.   U. R. Evans, J. E. O. Mayne, Protection by paints richly pigmented with Zn dust. *Society of Chemical Industry Journal* **1944**, *22*, 109-110.

7.   S. Feliu, R. Barajas, J. M. Bastidas, M. Morcillo, Mechanism of cathodic protection of zinc-rich paints by electrochemical impedance spectroscopy. I. Galvanic stage. *Journal of Coatings Technology* **1989**, *61* (775), 63-69.

8.   S. Feliu, R. Barajas, J. M. Bastidas, M. Morcillo, Mechanism of cathodic protection of zinc-rich paints by electrochemical impedance spectroscopy. II. Barrier stage. *Journal of Coating Technology* **1989**, *61* (775), 71-76.

9.   D. Battocchi, A. M. Simões, D. E. Tallman, G. P. Bierwagen, Electrochemical Behavior of a Mg-rich Primer in the Protection of Al alloys. *Corrosion Science* **2006**, (48), 1292-1306.

10.   G. P. Bierwagen, D. Battocchi, A. Simões, A. Stamness, D. Tallman, The use of multiple electrochemical techniques to characterize Mg-rich primer for Al alloys. *Progress in Organic Coatings* **2007,** (59), 172-178.

11.   C. A. Gervasi, A. R. Di Sarli, E. Cavalcanti, O. Ferraz, E. C. Bucharsky, S. G. Real, J. R. Vilche, The corrosion protection of steel in sea water using zinc-rich alkyd paints. An assessment of the pigment-content effect by EIS. *Corrosion Science* **1994,** *36,* 1963-1972.

12.   D. Battocchi, A. M. Simões, D. E. Tallman, G. P. Bierwagen, Comparison of Testing Solutions on the Protection of Al-alloys Using a Mg-rich Primer. *Corrosion Science* **2006,** *48,* 2226-2240.

13.   A. Simões, D. Battocchi, D. Tallman, G. P. Bierwagen, Assessment of the Corrosion Protection of Aluminium Substrate by a Mg-Rich Primer: EIS, SVET snf SECM Study. *Journal of Electrochemistry Society* **2008,** *155,* E143-E149.

14.   G. P. Bierwagen, C. J. Jeffcpate, J. Li, S. Balbyshev, D. E. Tallman, The Use of Electrochemical Noise Methods to Study Thick, High Impedance Coatings. *Progress in Organic Coatings* **1996,** *29,* 21-30.

15.   D. J. Mills, S. Mabbutt, Investigation of defects in organic anti-corrosive coatings using electrochemical noise measurement *Progress in Organic Coatings* **2000,** *39* (1), 41-48.

16.   S. Mabbutt, D. J. Mills, C. P. Woodcock, Development of the electrochemical noise method (ENM) for more practical assessment of anti-corrosion coatings. *Progress in Organic Coatings* **2007,** *59,* 192-196.

17.   H. A. A. Al-Mazeedi, R. A. Cottis, A practical evaluation of electrochemical noise parameters as indicators of corrosion type. *Electrochimica Acta* **2004,** *49,* 2787-2793.

CHAPTER 5. RESULTS AND DISCUSSION OF MECHANICAL MEASUREMENTS

5.1. Abstract

The mechanical properties and chemical resistance property of the flexible Mg-rich coating were measured and compared with the traditional epoxy based Mg-rich coating from Akzo Nobel Co. by several empirical laboratory coating testing methods in this study, which include conical mandrel bending test, reverse impact resistance test and solvent resistance test (a.k.a. MEK double-rub). DMTA was also used to quantitatively investigate the flexibility of the Mg-rich coatings, especially the dynamic and static moduli at low temperature. All the data have indicated that the sulfur-containing Mg-rich coating is more flexible. The relationship between the weathering time and the Mg-rich coatings' flexibility was also investigated by the nano-indentation technique. Based on the results, it was found that the Mg-rich coatings' mechanical properties were comprehensively controlled by post curing of the polymeric coatings; the water diffusing into the Mg-rich primer to plasticize the polymer; the formation of Mg oxides, which is harder than pure magnesium; and the aging of the polymers.

5.2. Introduction

The coating system of military aircraft must protect the aluminum structure and associated fastening and joining mechanisms from corrosion in a variety of aggressive environments. Excessive grinding is often needed to remove the corrosion products at the

48

cracks formed around the seams and fasteners on the aircraft resulting from poor system flexibility of coatings, which causes high maintenance cost and damages the integrity of an aircraft' s body.[1] Thus, the Air Force wants to develop an advanced performance coating system with a primer that can provide superior flexibility, good corrosion protection, and low volatile organic compound emissions, all of which are considered as key performance parameters in the new military specifications of the Air Force.

Currently, commercialized Mg-rich corrosion protection primers are generally brittle coatings developed from some epoxy-amine coating systems. The epoxy-based coatings have good performance in nearly all aspects but flexibility, despite the enhancement made by designing the epoxy-based Mg-rich primers with low cross-link density. Therefore, an elastomer-modified epoxy coating would be a desirable alternative for the binder of Mg-rich primers.

Polysulfides were found to be a good elastomer as the replacement of natural rubber in some application where good chemical resistance is needed. A typical $-S_x-$ bond in polysulfides provides the polymer backbone with a lower rotation energy threshold than carbon-carbon single bond, which means more flexibility and pliability.

In this research, TZ 904, a sulfur-containing sealant manufactured by Chevron Phillips Chemical Company L.P., was examined as a binder of Mg-rich primer based on its superior flexibility. The ultimate mechanical properties, such as elongation ratio, dynamic and static modulus, and hardness, were investigated by mandrel bending tests, impact resistance tests, DMTA and nano-indentation to identify how the flexibility of the sulfur containing Mg-rich primer is improved, compared with the standard epoxy based aerospace

Mg-rich coating. In addition, the relationship between the Mg-rich coatings' flexibility and laboratory accelerated weathering was also examined.

5.3. Experiment

5.3.1. Empirical Tests

ASTM D 823-95 (Standard Practices for Producing Films of Uniform Thickness of Paint, Vanish, and Related Products on Test Panels) was used as the basis for sample preparation. Three sulfur-containing Mg-rich primers with different PVCs (30%, 40%, and 50%) were sprayed on Q-PANEL® QD-35 steel panels (0.02''×3''×5'') with 1 mil wet thickness, as well as Akzo Nobel aerospace Mg-rich epoxy primer that has a PVC of 45%. Then each type was coated by three kinds of topcoats: 03-GY-277 (high gloss polyester-isocyanate topcoat by DEFT), 03-GY-310 (low gloss polyester-isocyanate topcoat by DEFT), and 646-58/X501 (white enamel epoxy-polyurethane topcoat by Akzo Nobel). Three parallel samples were made for each topcoat /primer system, as well as non-topcoated primer system. The coatings' elongation ratios can be determined from the tests according to ASTM D 522-93a (Standard Test Methods for Mandrel Bend Test of Attached Organic Coatings).

For impact resistance and chemical resistance tests, all primers were applied on Q-PANEL® 3003H14 aluminum panels which were rinsed and cleaned by hexane as instructed by ASTM D 823-95, and these samples were repeatedly tested without any topcoats based on ASTM D 6905-03 (Standard Test Methods for Impact Flexibility of

Organic Coatings) and ASTM D 5402-93 (Standard Practice for Assessing the Solvent Resistance of Organic Coatings Using Solvent Rubs).

The thicknesses were measured by an elcometer before testing. Table 2 is for average thicknesses and standard deviations of all the films, w/ and w/o topcoat. It demonstrates that the dry thicknesses were found to increase even if the coatings were applied in a uniform wet thickness as PVC is increased.

Table 2. Average thicknesses and standard deviations of the whole films w/ and w/o topcoat films.

PVC	Non-topcoated		High gloss		Low gloss		White enamel	
	x(mm)	σ	x(mm)	σ	x(mm)	σ	x(mm)	σ
30%	45	6.1	56	4.0	64	4.3	69	7.8
40%	47	3.3	69	7.5	71	4.7	66	5.9
45%	48	3.8	76	6.1	82	8.1	75	6.5
50%	63	4.2	87	11.0	108	12.1	86	6.7
Akzo Nobel	45	2.4	79	10.0	86	11.8	80	7.2

5.3.2. DMTA Experiments

Since the highly pigmented coatings are too brittle to undergo tensile tests as ASTM D 2370-98 (Standard Test Methods for Tensile Properties of Organic Coatings), the Mg-rich primers were cast on the DuPont™ Tedlar® polyvinyl fluoride (PVF) films supported by a glass panel. After cured and carefully peeled off from PVF film, the free Mg-rich coating films were cut into 25mm×5mm specimens to evaluate through DMTA. These specimens should not exhibit any nicks or flaws that can be found by the naked eye. TA Instruments DMA Q800 was deployed to test the specimens to get both dynamic and static

mechanical properties. Under "controlled force" mode, a constant-rate-of-crosshead-movement type of extension was applied on the testing specimens at -50°C and room temperature with a suitable force ramping to determine the static mechanical properties, while the dynamic modulus and the tan δ were obtained at the single frequency of 1 Hz in "multi-frequency-strain" mode with temperature ranging from -100°C to about 250°C.

5.3.3. Nano-Indentation Technique to Study Weathering Impact

The nano-indentation test, which is used to investigate mechanical properties in micro- or nano- scale, was carried out by Hysitron Triboscope with a Berkovich tip in this experiment. A "5-5-5" trapezoid-shaped load function demonstrated in Figure 13 (loading 5 sec. to peak force, maintaining peak force for 5 sec., unloading 5 sec.) with peak forces of 500μN, 1000μN, 1500μN and 2000μN was respectively mounted on the samples underneath the tip.

The sulfur-containing flexible Mg-rich primers of different PVCs (30%, 40%, and 45%) and Akzo Nobel aerospace Mg-rich primer that is used as the reference standard were sprayed on pretreated AA 2024-T3 panels according to ASTM D 823-95, and topcoated by Akzo Nobel white gloss urethane topcoat 646-58-7925. Then all the coated samples were divided into two groups and placed in the B117 salt spray chamber. Nevertheless, two issues are needed to be considered before using nano-indentation technique to characterize the mechanical properties of the Mg-rich primers: first of all, the topcoat has to be removed to let the indenter reach the surface of the Mg-rich primers when testing; second, the surface of spontaneously formed Mg-rich primer films is much too rough to cast the nano-scaled indenter. Based on these two considerations, Leica SM2500 microtome with a

tungsten carbide blade was deployed to section out a relatively smooth surface from the primer films with an angle of 1.9° to the Al alloy substrate surface which was anchored by a two-sided tape to a high density polypropylene cutting block (See Figure 14). In such a way, the Mg-rich primer films with an exposed smooth surface were ready to take nano-indentation tests.
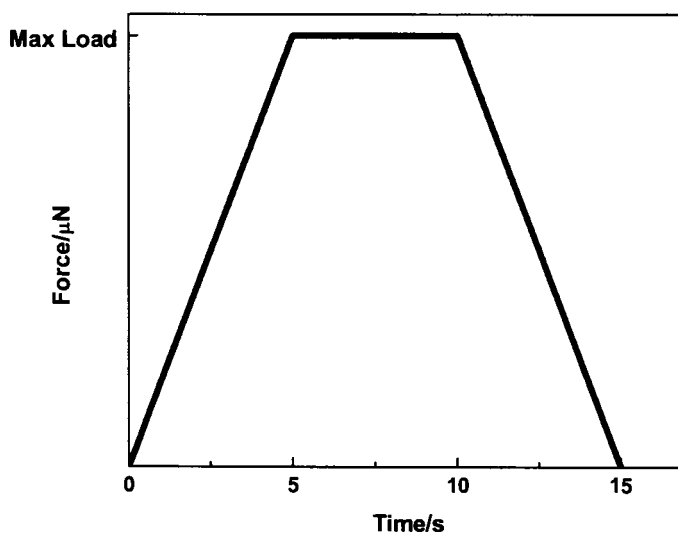

Figure 13. Illustration of the force-time relation in the trapezoid-shaped load function.

As the objective of this research, the binders of the Mg-rich primers, both the sulfur-based and the standard, were indented twelve to sixteen times to get an average value of hardness along with reduced moduli. Given there could be voids or pigments underneath the surface in the pigmented primer system, even though indents were made on the polymeric binder based on the observation of the microscope on the instrument, repeated measurements were necessary to diminish such kinds of system errors.

5.4. Results and Discussion

5.4.1. Conical Mandrel Bending Experiments

The conical mandrel bending tests were carried out according to ASTM D 522-93a, and the lengths of cracks were recorded for each panel (shown in Figure 15). Elongation rates in Table 3 were obtained based on the converting graph from ASTM shown in Figure 5. Pure primer panels show perfect cracking resistance under mandrel bending test, since the results of non-topcoated coating samples can be converted into $\geq 32\%$ elongation value. And it can also be observed that increasing PVC slightly decreases the flexibility of coatings.
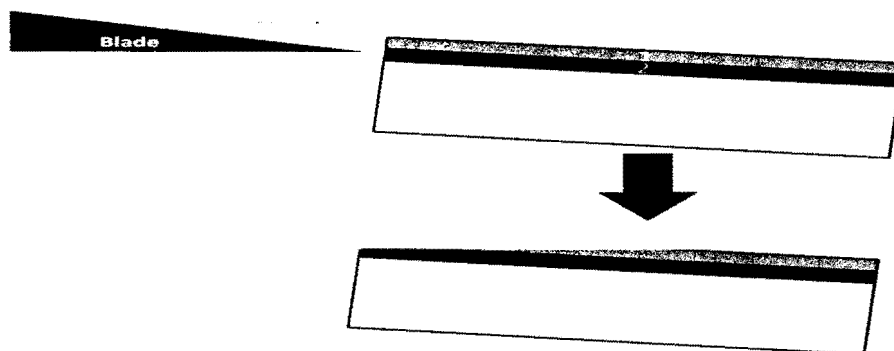

Figure 14. Schematic depicting the concept of sample preparation for nano-indentation measurement. 1 stands for topcoat, 2 for Mg-rich primer.

Table 3. Elongation rates converted from length of cracks.

PVC	Non-topcoated			High gloss			Low gloss			White enamel		
	1	2	3	1	2	3	1	2	3	1	2	3
30%	≥32%	≥32%	≥32%	≥32%	≥32%	≥32%	≥32%	≥32%	≥32%	≥32%	≥32%	≥32%
40%	≥32%	≥32%	≥32%	≥32%	31%	≥32%	31%	≥32%	≥32%	≥32%	≥32%	≥32%
50%	≥32%	≥32%	≥32%	≥32%	≥32%	≥32%	29%	30%	24%	29%	≥32%	≥32%
AN*	20%	24%	21%	22%	31%	17%	17%	20%	19%	8%	14%	16%

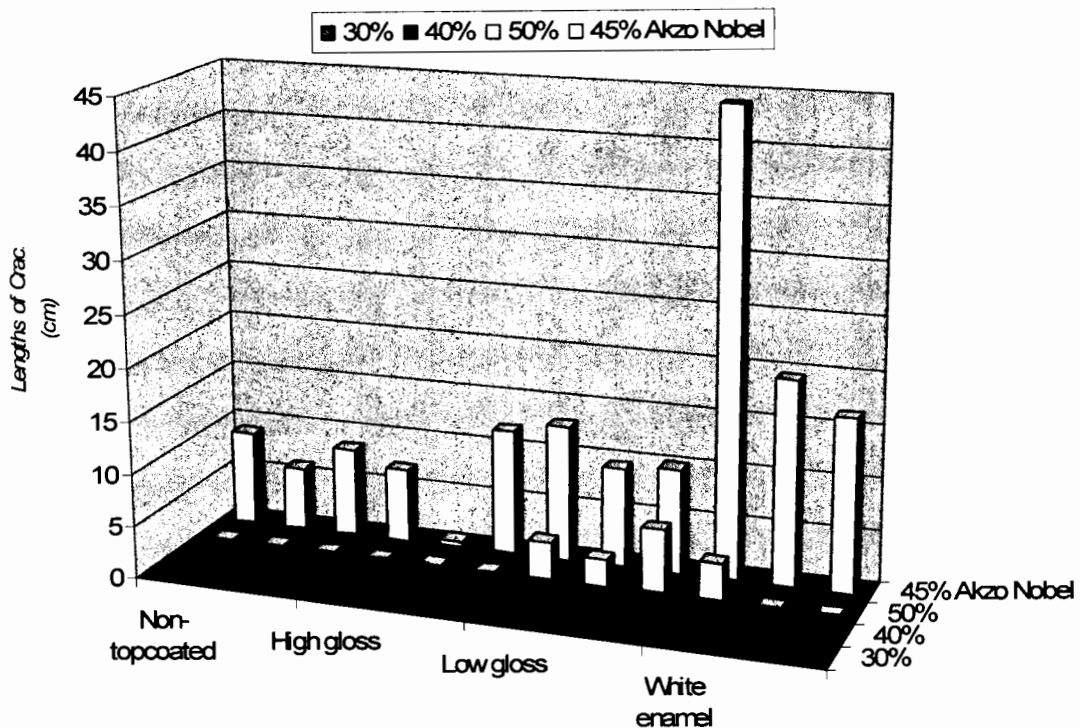*: Akzo Nobel Mg-rich epoxy primer, PVC is 45%

Figure 15. 3-D column bar-chart of conical mandrel bending tests.

The flexible Mg-rich primer provides remarkable improvement on bending tests compared with Akzo Nobel non-flexible epoxy primer, and the flexible primer with even higher PVC has a much better appearance than the ordinary epoxy primer.

It can be concluded that the cracks are mainly due to the failure of topcoats under bending for the flexible primers, because the flexible primers with a variety of PVCs by themselves showed a $\geq 32\%$ elongation rate, while the elongation value was decreased after the primers were topcoated. The superior flexibility of the primer and good adhesion to topcoats helps the topcoat/primer system withstand the bending tests.

5.4.2. Reverse Impact Resistance Experiments

As instructed by ASTM D 6905-03, test results were recorded in Table 4. The 40% PVC sulfur containing Mg-rich primer has the best performance above all. Compared with the standard Mg-rich primer from Akzo Nobel Co. with a PVC of 45%, the sulfur-containing flexible Mg-rich primer with the same PVC is more flexible and more resistant to reverse impact.

Table 4. Reverse impact test results.

Primer	5%[*]	30%	40%	45%	50%	AN[**]
Impact resistance (in×lb)	20.4	22	26.8	17.6	6	12

[*]: 5% PVC counts on TiO_2 pigment that already exists in the product when obtained.

[**]: Akzo Nobel Mg-rich epoxy primer, PVC is 45%

5.4.3. Solvent Resistance Experiments

Solvent resistance is not a mechanical property, but it is included here because it is one of the coating properties that must be balanced with mechanical properties for some applications. The solvent resistance of aerospace coatings is desired due to its exposure to jet fuels, lubrication oils, and so on, comprehensively creating an aggressive application environment for aerospace coatings. MEK double-rub tests were carried out to evaluate solvent resistance property of the Mg-rich primers according to the testing procedure from ASTM D 5402-93. Since coating film thicknesses have a dramatic impact on MEK double-rub test results, they are also presented in the brackets following the test results in Table 5.

The existence of pigment particles obviously compromises the coatings' solvent resistance which decreases along with the increasing PVC. But even so, the sulfur-containing flexible Mg-rich primer appears to be slightly more solvent resistant than the Akzo Nobel Mg-rich primer at the same PVC.

Table 5. MEK double rub test results.

Primers	1	2	3
5%	>200 (50μm)	182 (32μm)	>200 (41μm)
30%	>200 (66μm)	139 (43μm)	159 (48μm)
40%	112 (54μm)	100 (51μm)	115 (52μm)
45%	102(74μm)	111(68μm)	92(62μm)
50%	70 (92μm)	105 (141μm)	106 (132μm)
AN	89 (70μm)	56 (54μm)	72 (58μm)

5.4.4. DMTA Experiments

Because aircraft coatings have, perhaps, the widest temperature range among use of all high performance coatings, it implies that the desired flexibility of the aircraft coatings must hold over this temperature range, and therefore be tested over this range. DMTA is quite useful for testing aerospace coating systems at different temperatures. Dynamic mechanical thermal analysis of each cured system was conducted in the research to investigate the elastic and viscoelastic behavior of the polymeric coating films. Tan δ vs. temperature, storage modulus E' vs. temperature and loss modulus E" vs. temperature are given respectively in Figure 16, Figure 17, and Figure 18. Tan δ equals the quotient of the

57

loss modulus, E", divided by the storage modulus, E'. In each case of Figure 16, the peak represents the glass transition temperature, T_g, measured by the DMTA technique. For the same binder, an increase in pigmentation usually causes an increase of T_g to higher temperature.[2] When the comparison is made between samples made of different polymeric materials, empirically, higher T_g indicates greater inflexibility and hardness. Moreover, the moduli of particulate polymeric composites are normally higher than those of homogeneous polymeric materials perhaps due to polymer-filler bonding.[3, 4] Figure 17, therefore, suggests that the sulfur-containing flexible Mg-rich coating becomes more rigid with the increasing volume percentage of Mg pigment. But when the flexible coating's PVC reaches 45%, as high as Akzo Nobel aerospace Mg-rich primer, the T_g is still lower than that of the latter. A combination of analysis of Figures 17 and 18 shows that at low temperatures (-100°C to 0°C) the sulfur-containing Mg-rich coatings with PVCs of 40% and 45% have higher dynamic moduli, which means they are more capable to dissipate energy (E") and store energy (E'), instead of resulting in cracks, than the standard Mg-rich coating.

The tensile strength of films generally increases with PVC to a maximum at CPVC but then decreases above CPVC.[2] But in this research, the reduction of tensile strength, as well as elongation-at-break, from low PVC to high PVC indicates the increasing inflexibility caused by Mg pigment particles; see Figure 19. It can also be noticed that the Young's modulus is increasing with the addition of Mg pigment which is harder than the polymer matrix. Comparing the plot of Figure 20 with the plot of the 45% PVC sulfur-containing Mg-rich coating in Figure 19, the flexibility of the 45% PVC sulfur-containing Mg-rich primer is higher than the standard Mg-rich primer at room temperature. Figures 21

58

and 22 illustrate the sulfur-containing Mg-rich primers' low temperature's stress-strain curves at -50°C based on the experiments carried out with load ramp of 0.4N/min and 0.05N/min, respectively. As expected, the Mg-rich coatings are more inflexible and stiffer at -50°C, showing higher Young's moduli, lower tensile strength, and lower elongation-at-break. The inflexibility of AN Mg-rich primer resulted in even lower load ramp applied: 0.025N/min.
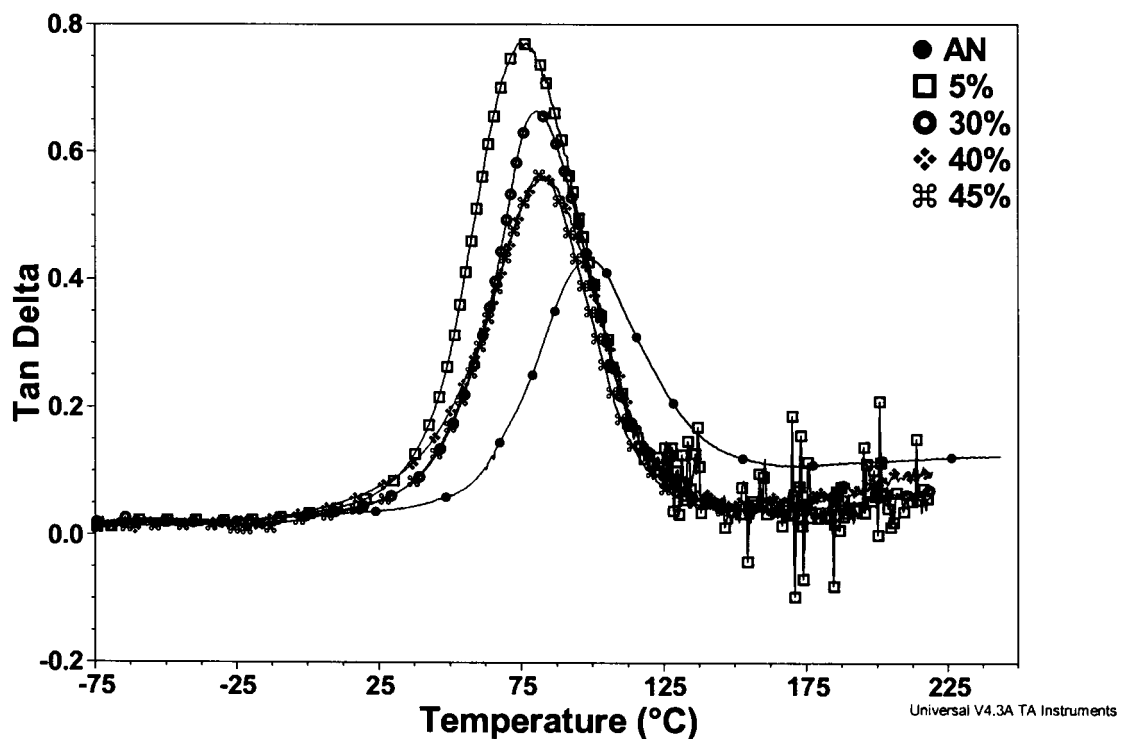

Figure 16. Measurements of tanδ of the Mg-rich primers; the legend from top to bottom: 40% PVC Mg-rich primer; standard Mg-rich primer; 5% PVC Mg-rich primer; 30% PVC Mg-rich primer; 45% PVC Mg-rich primer.
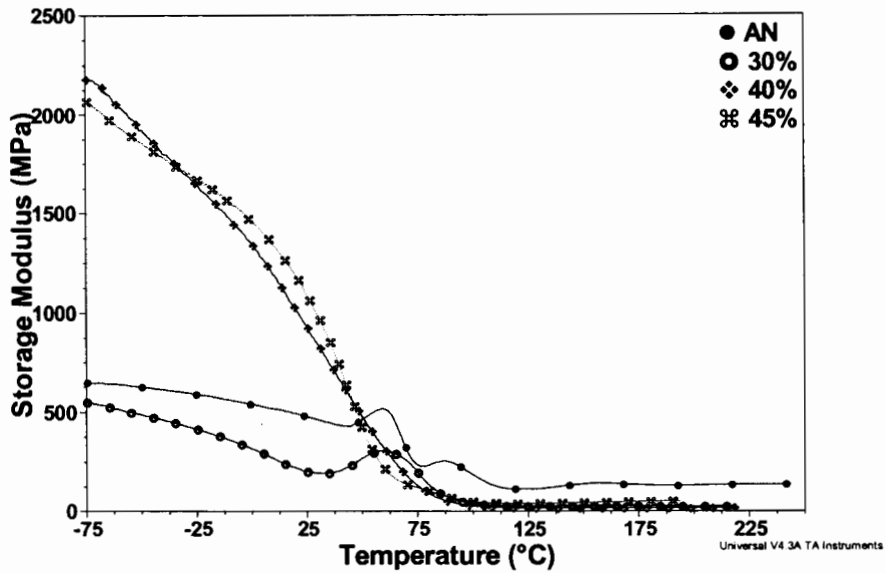
5.4.5. Nano-Indentation Experiments

Figure 17. Measurements of storage modulus of the Mg-rich primers; the legend from top to bottom: 40% PVC Mg-rich primer; standard Mg-rich primer; 30% PVC Mg-rich primer; 45% PVC Mg-rich primer.
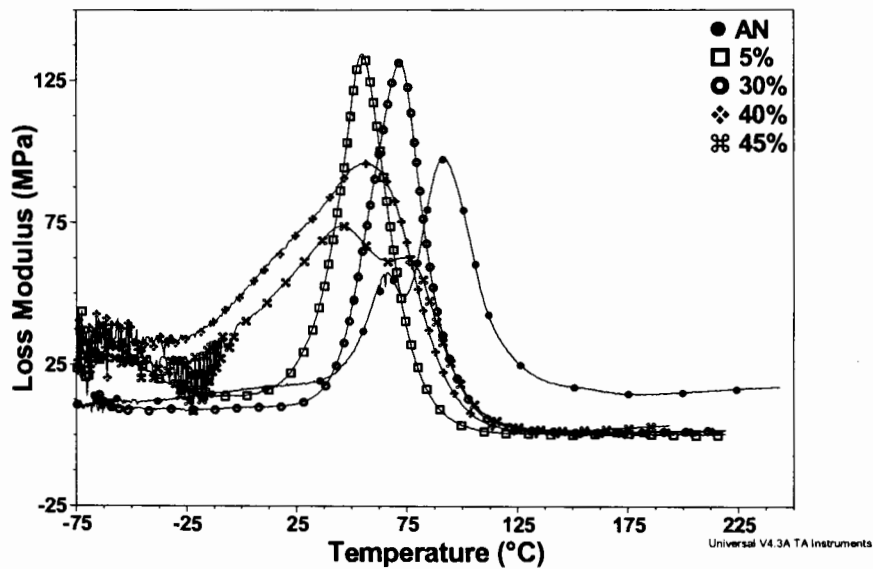

Figure 18. Measurements of loss modulus of the Mg-rich primers; the legend from top to bottom: 40% PVC Mg-rich primer; standard Mg-rich primer; 30% PVC Mg-rich primer; 45% PVC Mg-rich primer.
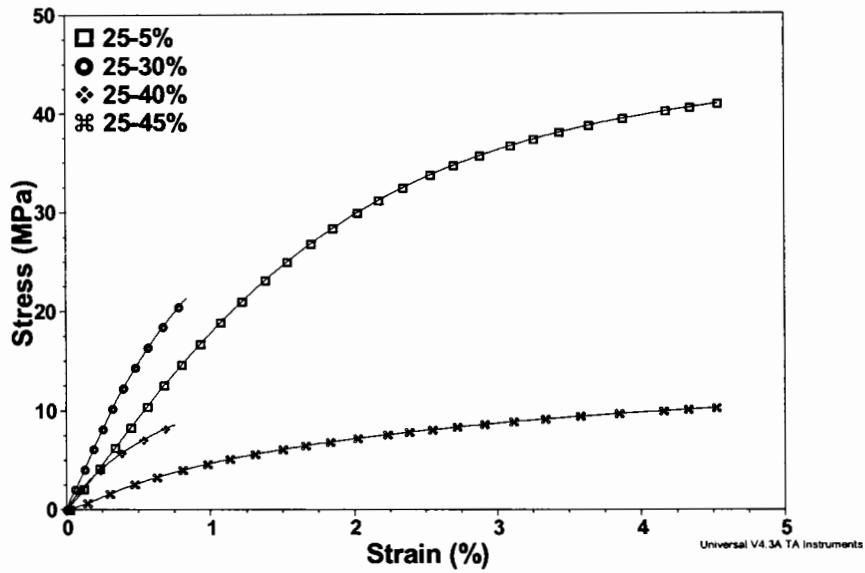
60

Figure 19. Stress-strain curves of the flexible Mg-rich coatings at room temperature. 45% PVC flexible primer films were measured at the load ramp 0.05N/min; 5%, 30% & 40% PVC primer films were measured at 0.4N/min.
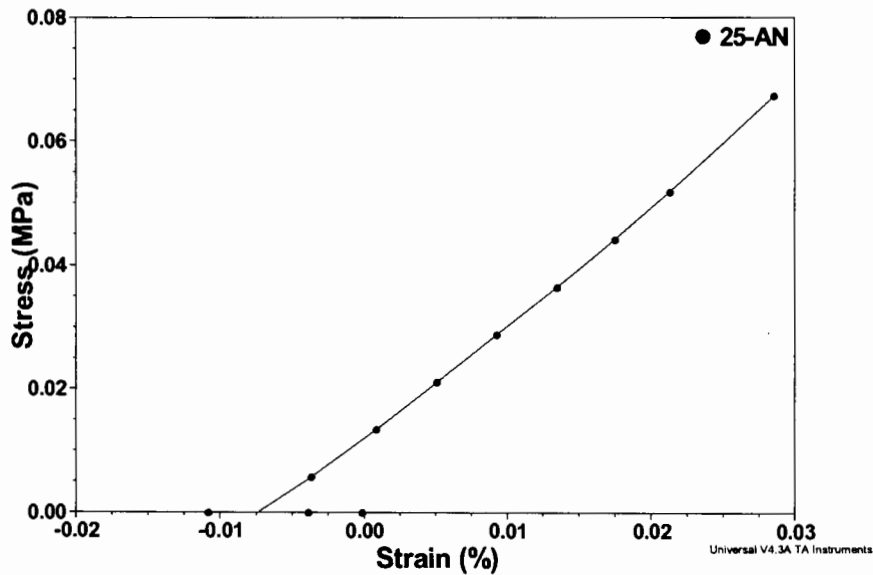

Figure 20. Stress-strain curves of the inflexible standard Mg-rich coatings at room temperature. They were measured at the load ramp 0.05N/min.
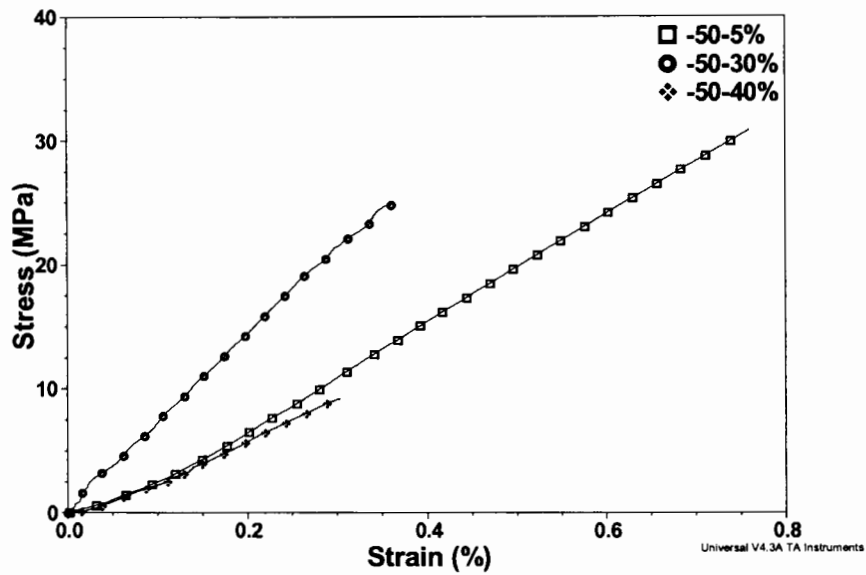
Figure 21. Stress-strain curves of the flexible Mg-rich coatings at-50°C. Data were collected at load ramp 0.05N/min.
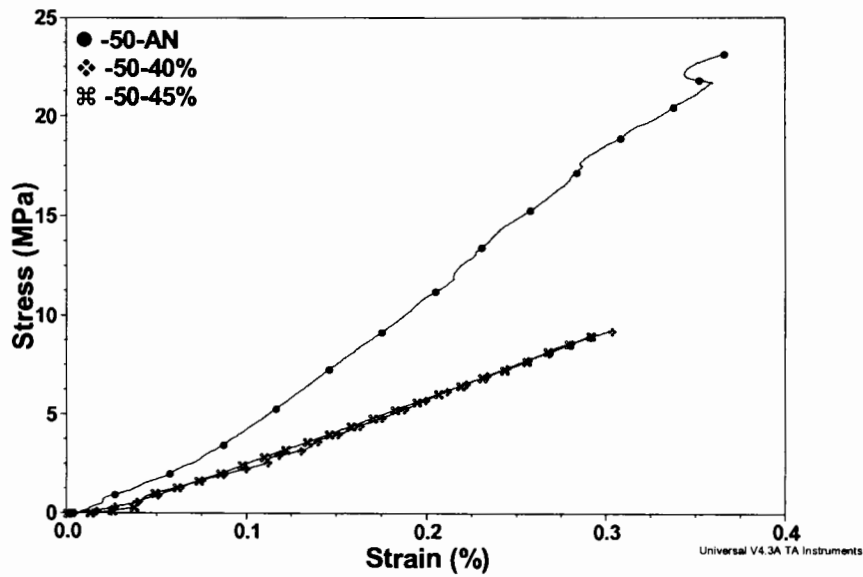

Figure 22. -50°C Stress-strain curves. Data were collected at load ramp 0.05N/min, but Akzo-nobel standard primer film's data were collected at 0.025N/min load ramp.

Before testing the Mg-rich coatings with the nanoindentation method, the pure polymeric materials that are included in the Mg-rich coatings and the Mg pigment were separated and respectively tested by the nano-indentation method. The averaged results listed in Table 6 indicate again the sulfur-containing coating's superior flexibility, given that its hardness and modulus are much lower than that of the standard aerospace coating's binder.

However, these initial results cannot be taken as evidence to prove the sulfur-containing polymer's anti-weathering capability. To research the effect of weathering on the mechanical properties of the flexible polymer in the Mg-rich coating system, the B117 salt spray accelerated weathering chamber was used as a workhorse again for the purpose of sample weathering. Besides the initial tests, samples were characterized by nano-indentation after 1st, 2nd, 4th, 6th, 9th, and 12th week exposures. Hardness and reduce modulus vs. exposure time are plotted respectively in Figures 23 and 24. A similarity can be observed from both Figures 23 and 24: there is an apparent increase occurring in each curve at the 2nd week, followed by a steady decrease, and then the curves resume increasing at the 6th week. Some researchers[5, 6] also found the increase of the mechanical properties after first short-time aging when using nanoindentation to characterize some polymers. The embrittlement effect is thought to result from the intermolecular recombination through the generation of crosslinked molecules. Moisture absorption in polymers usually causes plasticization and hydrolytic effects, so the modulus and glass transition temperature of many polymers are often reduced after moisture absorption.[6, 7] Therefore, four major factors could be involved to explain the circumstance: the post-cure of polymeric binders; the water diffusing into the Mg-rich primer to plasticize the polymer; the formation of Mg

oxide, which is harder than pure magnesium; and the aging of the polymers. It is apparent that the sulfur containing Mg-rich primer is more flexible than the reference standard during the entire weathering process.

Table 6. Elastic modulus and hardness of the binders and Mg pigment by nano-indentation.

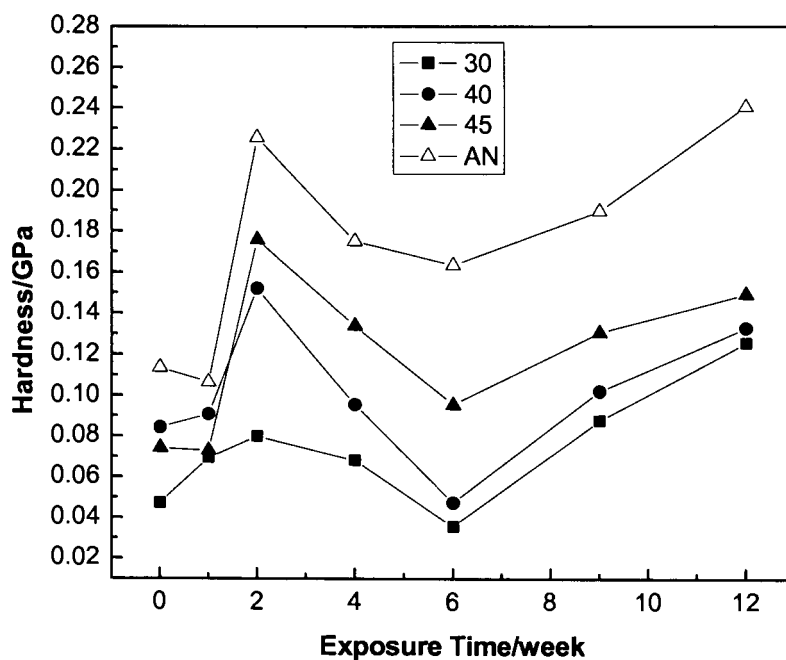|	Reduced Modulus (GPa)	Hardness (GPa)
Sulfur-containing flexible coating	0.40637	0.007485
AN aerospace coating	1.06672	0.0167
Mg pigment	27.35627	0.60596

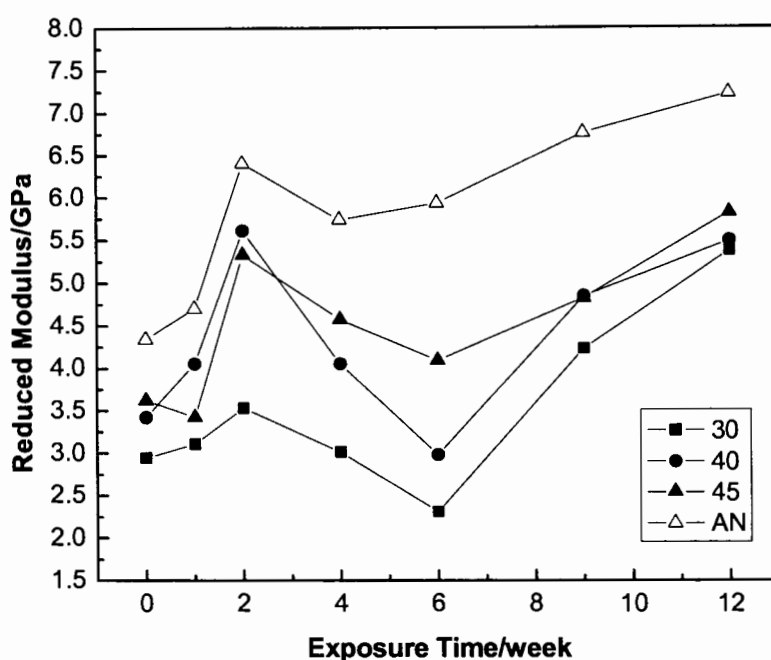Figure 23. Hardness vs. exposure time.

Figure 24. Elastic modulus vs. exposure time.

5.5. Conclusions

The flexibility of the sulfur based Mg-rich primer and the standard epoxy based Mg-rich primer were measured by DMA, nano-indentation, and some empirical laboratory methods. The superiority of the sulfur based coating has been shown in both mechanical properties and chemical resistance properties. The impact of weathering was also examined in this research, and it was shown that the flexibility of the Mg-rich primers from Akzo Nobel aerospace coatings and the sulfur-based polymer both fell upon exposure, but the sulfur-based polymer maintained its flexibility advantage through it.

5.6. References

1.   S., Mike, Advanced Performance Coating System: Polysulfide/APC Evaluation. 2003.

2.   Z. W. Wicks Jr., F. N. Jones, S. P. Pappas, D. A. Wicks, *Organic Coatings: Science and Technology, 3rd edition*. Wiley-Interscience: Hoboken, NJ, 2007.

3.   P. S. Theocaris, G. D. Spathis, Glass-transition behavior of particle composites modeled on the concept of interphase. *Journal of Applied Polymer Science* **1982,** *27* (8), 3019-3025.

4.   D. Y. Perera, Effect of pigmentation on organic coating characteristics *Progress in Organic Coatings* **2004,** *50* (4), 247-262.

5.   K. C. C. Tse, F. M. F. Ng and K. N. Yu, Photo-degradation of PADC by UV radiation at various wavelengths. *Polymer Degradation and Stability* **2006,** *91*, 2380-2388.

6.   R. S. C. Woo, H. Zhu, C. K. Y. Leung, J. Kim, Environmental degradation of epoxy-organoclay nanocomposites due to UV exposure: Part II residual mechanical properties. *Composites Science and Technology* **2008,** *68* (9), 2149-2155.

7.   X. Shi, S. G. Croll, Recovery of surface defects on epoxy coatings and implications for the use of accelerated weathering. *Progress in Organic Coatings* **2009,** *In Press*.

CHAPTER 6. SUMMARY AND CONCLUSIONS

In order to find a method to enhance the flexibility of the aerospace Mg-rich primer, a unique sulfur-containing polymer binder was introduced to mix with Mg pigment. The newly developed sulfur-containing Mg-rich coating was expected to have superior flexibility and corrosion protection property, as well as good chemical resistance.

Three sulfur-containing Mg-rich primers were made at different PVCs (30%, 40%, and 45%), and then send to two different laboratory accelerated weathering protocols: the B117 neutral salt spray weathering and the Prohesion/QUV alternating weathering. Akzo Nobel aerospace Mg-rich primer, used as the reference standard, was also weathered in the same way. The electrochemical corrosion characterization and visual inspections were weekly carried out on the Mg-rich coating systems during exposure.

The Prohesion/QUV protocol seems to be more aggressive to the Mg-rich coatings than the salt spray B117 method, because all the Mg-rich coatings from the Prohesion/QUV alternating protocol were seriously delaminated along the scribes which were completely covered by corrosion products during the 23 week exposure. By contrast, there was no delamination occurring on the samples from the B117 chamber; instead, a number of blisters, which only appeared on the 30% and 40% PVC Mg-rich coatings, and less corrosion products were observed. The difference between the corrosion mechanisms of the Prohesion/QUV alternating weathering and the B117 salt spray weathering can also be testified by the electrochemical data from this research: the coatings from the Prohesion/QUV alternating weathering have higher low frequency impedances modulus

but less negative OCPs, and the B117 continuous salt spray accentuated blistering, whereas cyclic salt spray emphasized filiform and undercut corrosion.

It can be concluded that 45% PVC sulfur-containing Mg-rich coating can provide the best corrosion protection among the entire sulfur-containing Mg-rich coatings for aluminum alloy substrate that went through laboratory accelerated weathering, which is also comparable to the commercialized reference standard of the same PVC from Akzo Nobel Comapny. Considering the simple formulation and formulating method of the sulfur-containing Mg-rich coatings, the accelerated weathering results were considerably satisfactory: the failure of the Akzo Nobel Mg-rich primer took place under the Prohesion/QUV weathering protocol just one week after the sulfur-containing Mg-rich coatings delaminated.

The mechanical properties between the two Mg-rich coatings were also measured and compared. Conical mandrel bend tests and reverse impact resistance tests characterize materials' flexibility in different ways: the bend tests focus on the coating's elongating and adhesion on substrate, while the impact tests are used to assess the ability of coating to withstand extension caused by rapidly applied force. In these two tests, as well as the solvent resistance test, the sulfur-containing Mg-rich coating was much superior to the traditional one at the same PVC level.

The dynamic and static moduli of the Mg-rich coatings were given by DMTA technique. Not only room temperature moduli were measured, but also the low temperature moduli that is more desired by the aerospace coatings. Even with high pigmentation, the DMTA results revealed that the sulfur-containing Mg-rich primers are still more flexible.

A relationship between the weathering time and the Mg-rich coatings' flexibility was investigated by nano-indentation. Hardness and modulus vs. the exposure time were plotted separately. Based on the plots, it was found that the topcoated Mg-rich coatings' mechanical properties were comprehensively controlled by the post cure of polymeric coatings; the water diffusing into the Mg-rich primer to plasticize the polymer; the formation of Mg oxides and release of metal ions that diffuse into polymer matrix; and the aging of the polymers. Each factor determines the mechanical properties in different periods.

Briefly, the sulfur-containing coating, when the magnesium pigment is dispersed in it, can perform as an anti-corrosion Mg-rich primer as well as the reference standard from Akzo Nobel Co.. In addition, the superior flexibility can make the sulfur-containing coating more desirable to be an aerospace Mg-rich primer. Based on the investigation results on the relationship between mechanical properties of Mg-rich coating and the weathering time by the nano-indentation method, the weathering impacts do not change the superiority of flexibility of the sulfur based Mg-rich primers.

Nevertheless, lots of future work can be done to improve the formulation of the sulfur-containing Mg-rich coating. On one hand, since much solvent was involved in the current formulation of the research, which causes the ideal situation of zero VOC coating unable to achieve, it suggests a new formulate method or some modification of the sulfur-containing polymer's structure to make itself less viscous. On the other hand, the TiO_2 pigment already existing in Chevron Phillips' sulfur-containing coating need to be diminished to fully exploit Mg pigment.